Characterisation of the *AT4G11100* gene, a negative regulator of disease resistance in *Arabidopsis thaliana.*

By Tyronne Kyle McCrindle

Dissertation presented for the degree of Master of Science in the Department of Molecular and Cellular Biology, at the University of Cape Town

February 2015

Supervisor: Dr Robert Ingle

Plagiarism Declaration

1. I know that plagiarism is wrong. Plagiarism is to use another's work and pretend that it is one's own.

2. I have used the Harvard convention for citation and referencing. Each contribution to, and quotation in, this report from the work(s) of other people has been attributed, and has been cited and referenced.

3. This report is my own work.

4. I have not allowed, and will not allow, anyone to copy my work with the intention of passing it off as his or her own work.

Signed by candidate

Signature Removed

..... 13/02/2015

Signature: Tyronne Kyle McCrindle Date

Acknowledgements

I would like to thank Dr Robert Ingle, my supervisor, for his invaluable support and guidance over the past three years. Without his confident direction, and consistent patience with the areas in which I struggled, this project would not have been possible. I am incredibly grateful for how approachable and encouraging he has been. I would also like to thank him for his repeated reading of my thesis (in its various iterations) and his detailed feedback; it really is very much appreciated.

I have received so much assistance and support from so many different people in the MCB department. Faezah Davids proved to be not only a fantastic teacher of protoplasts extraction techniques, but also a consistent source of general lab advice. Roslyn Ray, Alexis Bick, Madhu Chauhan, and Shakiera Sattar are just a few of the people who have lent some form of help at one time or another. Without the hard work from our lab's DA, Catherine, I think a lot more time would have been spent keeping the lab equipment clean, and a lot less time performing experiments. The MCB SuperCare staff also provided the invaluable service of keeping the entire building clean; I'd like to thank Pricilla and Eunice in particular for always greeting me with a smile.

I have loved my time in Lab 430. My lab mates are hilarious and create such a spirit of camaraderie that you can't help but enjoy your time there. A special thanks to Stacey, Emang, and Delroy; as the senior students in the lab when I joined they taught me so much and offered some great advice ("don't quote me on that!"). Jean and Tia have been such lovely companions, always there with a smile and happy to have a chat. Angus and Ed are

forever keen for a beer or an excited nerdy chat. Nicki Adams deserves especially warm thanks, she was always ready and willing to show me some or other technique, offer valuable advice on my project, transport me to or from varsity, or listen to the occasional vent. I'm going to miss working with all of you!

All my friends have made my experience in the department such a brilliant one; from tea time, to lunches, to Africa day, I've enjoyed (almost) every minute.

I would like to thank the National Research Foundation for their financial support throughout my postgraduate career at UCT. Their continued support of young scientists is commendable. The financial support from my parents also ensured that I could concentrate on my studies rather than worrying about how I was going to pay for fees/rent/food, and for that I'd like to offer my sincerest thanks.

Lastly I would like to thank Elizabeth Biney and Steven Bing for their continued love and support, you two really carried me through this whole thing.

List of Abbreviations

°C	degree Celsius
µ	micro
Avr	avirulence
bp	base pair(s)
cDNA	complementary deoxyribonucleic acid
cfu	colony forming units
cir1	constitutively induced resistance 1 mutant
Col-0	*Arabidopsis thaliana* ecotype Columbia
DEPC	diethylpyrocarbonate
DNA	deoxyribonucleic acid
dNTP	deoxynucleosidetriphosphate
DTT	dithiothreitol
EDTA	ethylenediamine tetraacetic acid
ETI	effector-triggered immunity
g	gram(s)
g	gravity constant (9.81 ms-1)
eGFP	enhanced green fluorescent protein
h	hour(s)
HR	hypersensitive response
JA	jasmonic acid
kb	kilobase(s)
KB	King's broth

l	litre(s)
LB	Luria Bertani
LRR	leucine-rich repeat
LUC	firefly luciferase reporter gene
PR-1::LUC	Col-0 plants harbouring a *PR-1::LUC* gene cassette
M	molar
MAPK	mitogen-activated protein kinase
MAPKK	mitogen-activated protein kinase kinase
MAPKKK	mitogen-activated protein kinase kinase kinase
min	minute(s)
mm	millimetre(s)
mRNA	messenger ribonucleic acid
NB	nucleotide binding
ng	nanogram(s)
nm	nanometer(s)
OD	optical density
PAMP	pathogen-associated molecular pattern
PCR	polymerase chain reaction
PR	pathogenesis-related
PRR	pattern recognition receptor
Pst DC3000	*Pseudomonas syringae* pv. *tomato* DC3000
PTI	PAMP-triggered immunity
R	resistance
RLK	receptor-like kinase

RLU	relative light units
RNA	ribonucleic acid
SA	salicylic acid
SAR	systemic acquired resistance
SDS	sodium dodecyl sulphate
s	second(s)
U	unit(s)
UTR	Untranslated region
UV	ultraviolet
V	Volt
v/v	volume per volume
w/v	weight per volume

Abstract

Plants have evolved a complex system of defence to prevent pathogen establishment. The *Arabidopsis thaliana cir1* (*constitutively induced resistance 1*) mutant displays enhanced resistance to infection by the virulent bacterial pathogen *Pseudomonas syringae* and constitutively expresses a number of defence genes. Evidence suggests that CIR1 is a negative regulator of plant immunity important in the absence of pathogen attack. Genetic mapping experiments indicate that *cir1* is located on the lower arm of chromosome 4 of *A. thaliana* and may be one of 8 known genes in the region. Analysis of T-DNA knockouts of these 8 genes suggests that *AT4G11100* is the mostly likely candidate for *CIR1*. This project established that the disease resistance phenotype of *cir1* is temperature dependent and linked to reduced plant growth. Genetic crosses between *cir1* and *at4g11100* T-DNA knockout mutants revealed that the mutants complement and therefore *AT4G11100* is not *CIR1*. However, like *cir1,* the *at4g11100* T-DNA knockout mutants display enhanced disease resistance. Over expression of *AT4G11100* leads to increased susceptibility to infection by *Pseudomonas syringae* (*Pst)* and reduced induction of the salicylic acid defence gene *PR2* following *Pst* infection, suggesting that *AT4G11100* may too be a negative regulator of immunity. Additionally, a plant line with exceptionally high *AT4G11100* expression levels displayed distinct leaf morphology, possibly implicating *AT4G11100* in leaf development. Unfortunately, efforts to determine the subcellular localisation of AT4G11100 were unsuccessful, potentially due to problems with the expression of an *AT4G11100::eGFP* fusion, or even the instability of the resulting fused protein. Thus AT4G11100 is a likely negative regulator of plant immunity, and the identity of *CIR1* remains unknown. Parts of this research have been recently published (Carstens, M., Mccrindle, T.K., Adams, N., Diener,

A., Guzha, D.T., Murray, S.L., Parker, J.E., Denby, K.J., *et al*. 2014. Increased Resistance to Biotrophic Pathogens in the Arabidopsis Constitutive Induced Resistance 1 Mutant Is EDS1 and PAD4-Dependent and Modulated by Environmental Temperature. *PLoS ONE*. 9(10):4–11.).

Table of Contents

List of Figures

List of Tables

Chapter 1: Introduction

Human population levels have dramatically increased over the last ten thousand years, and further growth is predicted to put the global population at between 9 and 11 billion by 2050 (Cohen, 2003). This growth will require that crop yields are improved in order to meet intensified food production targets. However, global food security is threatened by a number of factors, chiefly: high levels of poverty in the developing world, environmental degradation, climate change, and emergent plant pathogens (Godfray *et al*., 2010). Plant pathogens in particular are problematic, with more than 10% of the annual global crop harvest lost to pests and diseases (Strange & Scott, 2005) and microorganisms alone accounting for more than 200 billion $US worth of crop losses every year (Horbach *et al*., 2011). The lack of genetic diversity within crop species, and the continued practice of industrial scale monocultures, leaves many agriculturally important plants vulnerable to pathogen attack.

The development of transgenic plants able to resist infection by virulent pathogens has the potential to improve crop yields. It is therefore important to gain an understanding of the molecular mechanisms that underlie the interactions between plants and plant-pathogens. The convergence of studies of plant immunology and pathogen infectivity is central to elucidating how plant-pathogen interactions can be manipulated to enhance disease resistance (Dodds & Rathjen, 2010).

Plant immunity

To prevent pathogen establishment and disease, plants have evolved a complex system of defence. This defence system is analogous to the innate immune system present in vertebrates, but otherwise differs from animal immunity in a number of important ways. The most striking of these differences is that, unlike vertebrates, plants lack a circulatory system that would accommodate adaptive immunity, and so rely solely on an innate immune system (Boller & Felix, 2009).

The innate immune system involves the recognition of non-host (or non-self) entities. The ability of a plant species to resist infection by an entire pathogen species is called non-host resistance (Nuernberger & Lipka, 2005). Non-host resistance is the most common mechanism of plant defence, and enables protection against a wide range of pathogens by utilizing both preformed defences and inducible responses (Mysore & Ryu, 2004). The waxy cuticle and cell wall of epidermal cells, as well as actin microfilaments in the cytoskeleton, act as an effective barrier to pathogen entry into the intracellular space (Jones & Takemoto, 2004). Together with these physical barriers, the constitutive production of numerous antimicrobial enzymes and secondary metabolites make up the non-host preformed defence.

PAMP Triggered Immunity (PTI)

The inducible responses of non-host defence can be divided into two primary branches, each recognizing a different type of non-host molecule. The first response involves the recognition of highly conserved microbial proteins called pathogen associated molecular patterns (PAMPs) by transmembrane pattern recognition receptors (PRRs) (Zipfel & Felix,

2005). This recognition induces a receptor-mediated defence response known as PAMP triggered immunity (PTI), which is characterised by the activation of basal defence mechanisms that include the activation of mitogen-activated protein kinases (MAPKs), oxidative bursts, plant hormone production, and the expression of defence related genes (Felix & Boller, 2003).

The activation of initial MAPKs stimulates several MAPK signalling cascades. These kinase cascades act as important signalling mediators between pathogen sensors and cellular defence responses (Meng & Zhang, 2013), and work as part of a complex signalling network that leads to the biosynthesis of plant hormones (including salicylic acid, ethylene, and jasmonic acid) and the induction of *pathogenesis related* (*PR*) defence gene expression.

A commonly cited example of PTI is the detection of the flg22 peptide of bacterial flagellin by the PRR FLAGELLIN SENSING 2 (FLS2). The flg22 peptide is a highly conserved 22 amino acid region of the flagellin protein, the primary constituent of bacterial flagella, which are used by bacteria for locomotion (Gómez-Gómez & Boller, 2000). Following detection of flg22, FLS2 associates with the receptor like kinase (RLK) BRI1-ASSOCIATED RECEPTOR KINASE 1 (BAK1), forming a heterodimer that is thought to initiate MAPK signalling cascades (Meng & Zhang, 2013); although the exact components involved in this initiation are still unknown, it has been established that FLS2/BAK1 complex is important for the establishment of innate immunity (Chinchilla *et al*., 2007).

Relatively little is known about the fundamental molecular mechanisms connecting PRR activation to initiation of MAPK signal transduction, however, the importance of MAPK

signalling cascades in activating cellular defence responses is well established (Colcombet & Hirt, 2008). For instance, following flg22 detection in *A. thaliana,* two MAPK signalling cascades are activated, whereupon the sequential transfer of phosphate groups is initiated; phosphate groups are transferred from MAPK kinase kinases (MAPKKKs) to MAPK Kinases (MAPKKs) and then onto MAPKs, which go on to regulate immunity (Nakagami, Pitzschke & Hirt, 2005). The first of these cascades consists of MEKK1 (a MAPKKK), MKK4/MKK5 (two redundant MAPKKs), and MPK3/MPK6 (two redundant MAPKs), with MPK3/MPK6 positively regulating the defence response (Asai *et al*., 2002). Similarly, the second cascade involves phosphate transfer beginning with MEKK1, but then braches to MKK1/MKK2 (two redundant MAPKKs), and MPK4, with MPK4 positively regulating basal defence and negatively regulating resistance protein mediated effector triggered immunity (Zhang *et al*., 2012).

Effector Triggered Immunity (ETI)

Because PAMPs are highly conserved molecules that are not easily lost or modified, it is difficult for pathogens to evolve PAMPs that do not trigger PTI. Instead, pathogens have evolved effector molecules able to subvert PTI, resulting in effector-triggered susceptibility (ETS) of the host plant (Jones & Dangl, 2006). Effector producing pathogens are able to directly introduce (via the type III secretion system) a wide variety of effector molecules into host cells, some of which are protein kinase inhibitors that prevent MAPK signalling and thus downstream defence activation (Xiang *et al*., 2008); in this way effector producing pathogens are able to greatly enhance their virulence (Dodds & Rathjen, 2010). Other effectors, such as AvrPto from *P. syringae*, interact directly with the intracellular kinase

domains of the PRRs themselves, preventing the autophosphorylation that occurs following binding of their PAMP ligands, and thus blocking downstream signalling (Xiang *et al*., 2008).

Enhanced pathogen virulence has exerted a selective pressure on host plants leading to the evolution of plant resistance (R) proteins, many of which are nucleotide-binding and leucine-rich repeat (NB-LRR) proteins (Eitas & Dangl, 2010). NB-LRR proteins are divided into two categories based on the structure of the N-terminus; TIR-NB-LRRs contain an N-terminus homologous to the animal immune system Toll and interleukin 1 receptor (TIR), whereas CC-NB-LRRs contain an N-terminus that possesses a coiled coil (CC) domain (Dangl & Jones, 2001; Gómez-Gómez, 2004). R proteins, encoded by *R* genes, recognise specific effector molecules in a gene-for-gene manner and are able to induce effector triggered immunity (ETI) by re-activating the MAPK signalling cascades (Abramovitch & Martin, 2004; Oh & Martin, 2011). ETI constitutes the second branch of the inducible non-host defence response, and differs from PTI in that it elicits a rapid, amplified and often prolonged defence reaction characterised by a hypersensitive response (HR) and programmed cell death.

Although there are some cases of direct recognition and interaction between R proteins and effector molecules (Dodds *et al*., 2006), most R proteins recognise effectors indirectly, usually by detecting effector induced modifications of certain host proteins, often components of PTI. This indirect recognition is known as the guard hypothesis, and a well-studied example of the guard hypothesis involves the "guardee" RPM1 INTERACTING PROTEIN 4 (RIN4). Phosphorylation of RIN4 is induced by *P. syringae* effectors, AvrB or AvrRpm1, and this modification of RIN4 is detected by the NB-LRR protein RPM1, which is

able to elicit ETI (Mackey *et al*., 2003; Liu *et al*., 2011). A third *P. syringae* effector, AvrRpt2, actually cleaves RIN4, and the resulting degradation of RIN4 is recognised by a second NB-LRR protein, RPM2, which is in turn able to activate ETI (Mackey *et al*., 2003). In this scenario, RPM1 and RPM2 act as "guards" of RIN4 and are able to detect modifications induced by AvrB, AvrRpm1, or AvrRpt2.

Another defence strategy evolved by plants involves the use of "decoys" to interfere with pathogen effector function. In the case of flg22 detection by the FLS2 PRR, the AvrPto effector molecule has been identified as a PTI suppressor upstream of MAPK cascade activation (He *et al*., 2006). AvrPto is a protein kinase inhibitor that binds FLS2, inhibiting autophosphorylation and thereby suppressing the MAPK cascade that would lead to defence activation (Xiang *et al*., 2008). Two plant resistance proteins are involved in the perception of AvrPto, namely PTO, a serine/threonine kinase, and PRF, a NB-LRR protein (Lin & Martin, 2007). PTO and PRF have been shown to constitutively interact in a manner that prevents any downstream signal initiation via PRF; however, in the presence of AvrPto, the effector molecule binds to PTO (potentially in competition with FLS2) which releases PRF from its interaction with PTO, and allows for activation of ETI responses (Xing *et al*., 2007). Here, PTO is thought to act as a "decoy" by having a kinase domain structurally similar to that of FLS2. Thus, AvrPto binds to both FLS2 and PTO, but whereas binding to FLS2 inhibits plant defence induction, binding to the PTO "decoy" has the opposite effect and results in the activation of ETI (van der Hoorn & Kamoun, 2008).

PTI and ETI, through various signalling pathways, elicit the expression of *PR* genes that enhance host resistance to infection. The inducible responses from both these defence stages lead to a third and final layer of innate immunity, namely, systemic acquired resistance (SAR). SAR occurs when the expression of *PR* genes in infected tissue causes the expression of the same *PR* genes in uninfected distal tissue, thereby conferring enhanced resistance to the rest of the plant and protecting from secondary infection (Fu & Dong, 2013). SAR is controlled via the production of the salicylic acid (SA) immune signal, which is able to trigger wide-spread transcriptional reprogramming and expression of *PR* genes (Durrant & Dong, 2004).

Figure 1 illustrates the example of PTI induction via the detection of the flg22 peptide, the suppression of PTI through the introduction of bacterial AvrPto effector molecules, and the induction of ETI through R protein mediated detection of AvrPto.

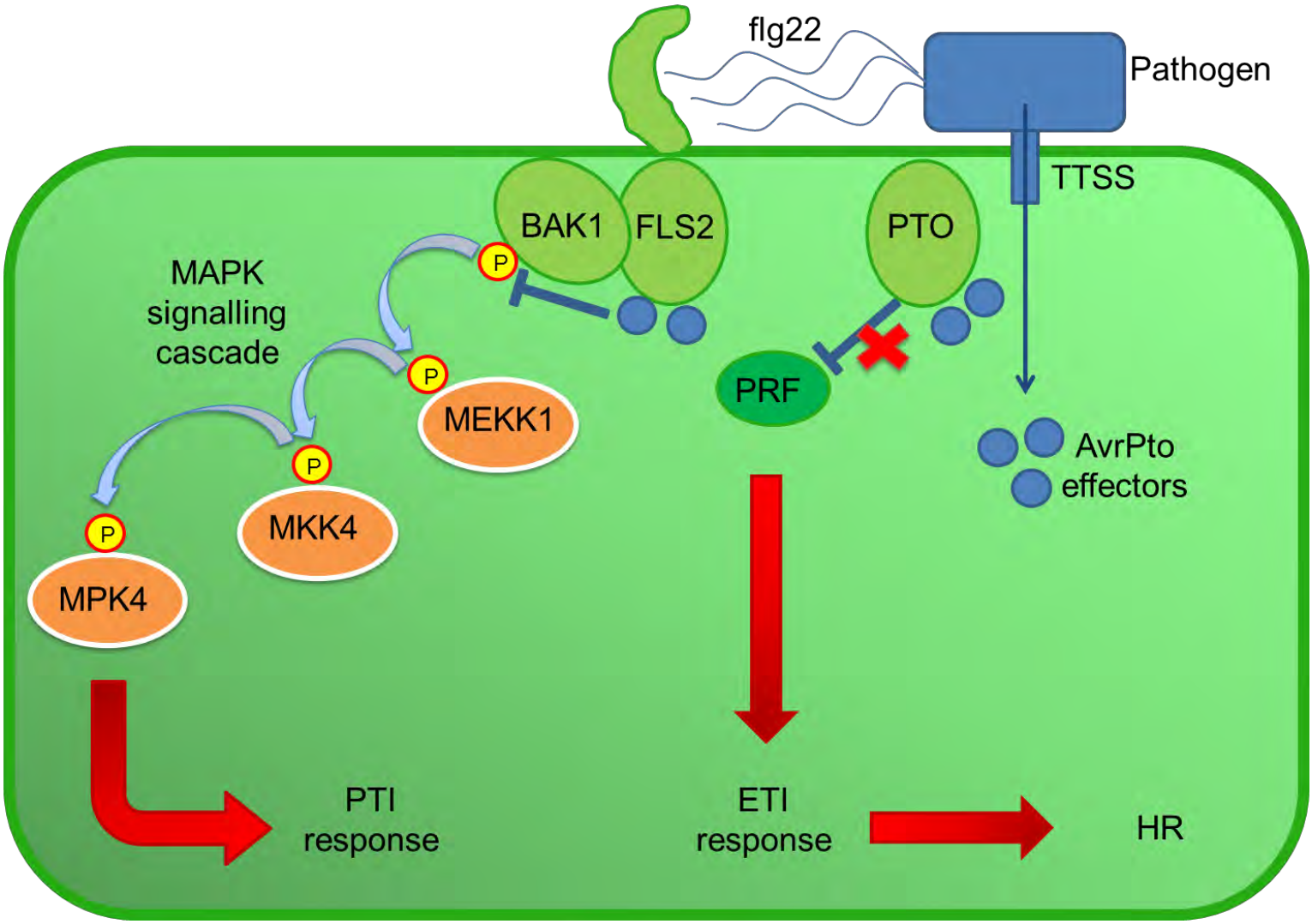

Figure 1| **An example of PAMP triggered immunity (PTI) and effector triggered immunity (ETI).** Detection of the flg22 pathogen associated molecular pattern (PAMP) by the FLAGELLIN SENSING 2 (FLS2) PAMP recognition receptor (PRR) triggers dimerization with BRI1-ASSOCIATED RECEPTOR KINASE 1 (BAK1) which initiates a cascade of mitogen-activated protein kinase (MAPK) signalling. MAPK signalling cascades lead to the induction of PTI through sequential transfer of phosphate groups. PTI is subverted by pathogen AvrPto effector molecules, introduced into the plant cell via the type three secretion system (TTSS). AvrPto prevents phosphorylation at the beginning of the MAPK cascade by binding to FLS2. ETI is induced when AvrPto effectors bind to the PTO serine/threonine kinase, which relaxes suppression of the PRF resistance (R) protein and leads to the activation of defence responses, including the hypersensitive response (HR).

Negative regulators of plant immunity

Plant defence responses are tightly controlled by a number of interconnected and complex networks of signalling pathways. These pathways interact in various ways to ensure appropriate defence responses are mounted to combat specific threats at specific times. Importantly, plants are able to supress immune responses in the absence of pathogens. Activation of defence is energetically expensive and can have detrimental effects on overall plant health; for example, a number of mutants with constitutively active defence responses, including *constitutive expressor of PR genes 1* (*cpr1*), *suppressor of npr1-1, constitutive 1* (*snc-1*), and *suppressor of rps4-RLD 1* (*srfr1*), display stunted growth and reduced reproductive capabilities (Zhang *et al*., 2003; Gou *et al*., 2009; Kim *et al*., 2010).

There are numerous proteins involved in the negative regulation of plant immunity; one such is the kinase-associated protein phosphatase (KAPP), which is able to bind to the kinase domains of a number of PRRs (including FLS2) and hinder autophosphorylation and downstream MAPK activation (Gómez-Gómez, Bauer & Boller, 2001). KAPP is an example of a moderator of the initial PTI, down-regulating this response once pathogen attack has abated.

Many of the key negative regulators of immunity work via controlling degradation of their target proteins. For example, NON-EXPRESSER OF PR GENES 1 (NPR1) is required for SA-induced *PR* gene expression during defence (Dong, 2004), and in the absence of SA, NPR1 is bound by its paralogue NPR4 which marks it for degradation by the proteasome (Fu *et al*., 2012). NPR4 is an adapter protein of the Cullin 3 (CUL3) E3 ligase which is able to mediate the degradation of its substrate (NPR1) in a SA dependent manner. In the absence of SA,

NPR1 is bound by NPR4, but when SA is present it will bind NPR4, reducing its affinity for NPR1 and thereby enabling NPR1 to activate signalling. NPR4 therefore acts as a negative regulator of immunity in the absence of pathogen attack by degrading NPR1 and preventing *PR* gene expression.

A negative regulator of ETI has already been discussed; the PTO kinase supresses ETI in the absence of pathogen introduced effector molecules by constitutively interacting with and deactivating the PRF NB-LRR protein (Xing *et al*., 2007). A similar example involves the MPK4 MAPK, which (as mentioned above) positively regulates basal defence *but* negatively regulates R protein mediated ETI (Zhang *et al*., 2012). Here, the PTI MAPK cascade is targeted by the HopAI1 effector molecule, which binds and inactivates MPK4. However, the inactivation of MPK4 relaxes the suppression MPK4 exerts on the NB-LRR protein SUMM2, leading to activation of ETI. In this way it is possible for a plant to modulate its defence response in the presence of PAMPs but not effector molecules, ensuring that only PTI is induced and the HR is avoided.

Figure 2 illustrates the examples mentioned above; these negative regulators form part of greater regulatory networks that, together, enable plants to finely control defence activation. Negative regulators of immunity are vital for suppressing defence in the absence of pathogens, and counteracting the fitness costs of constantly mounting immune responses.

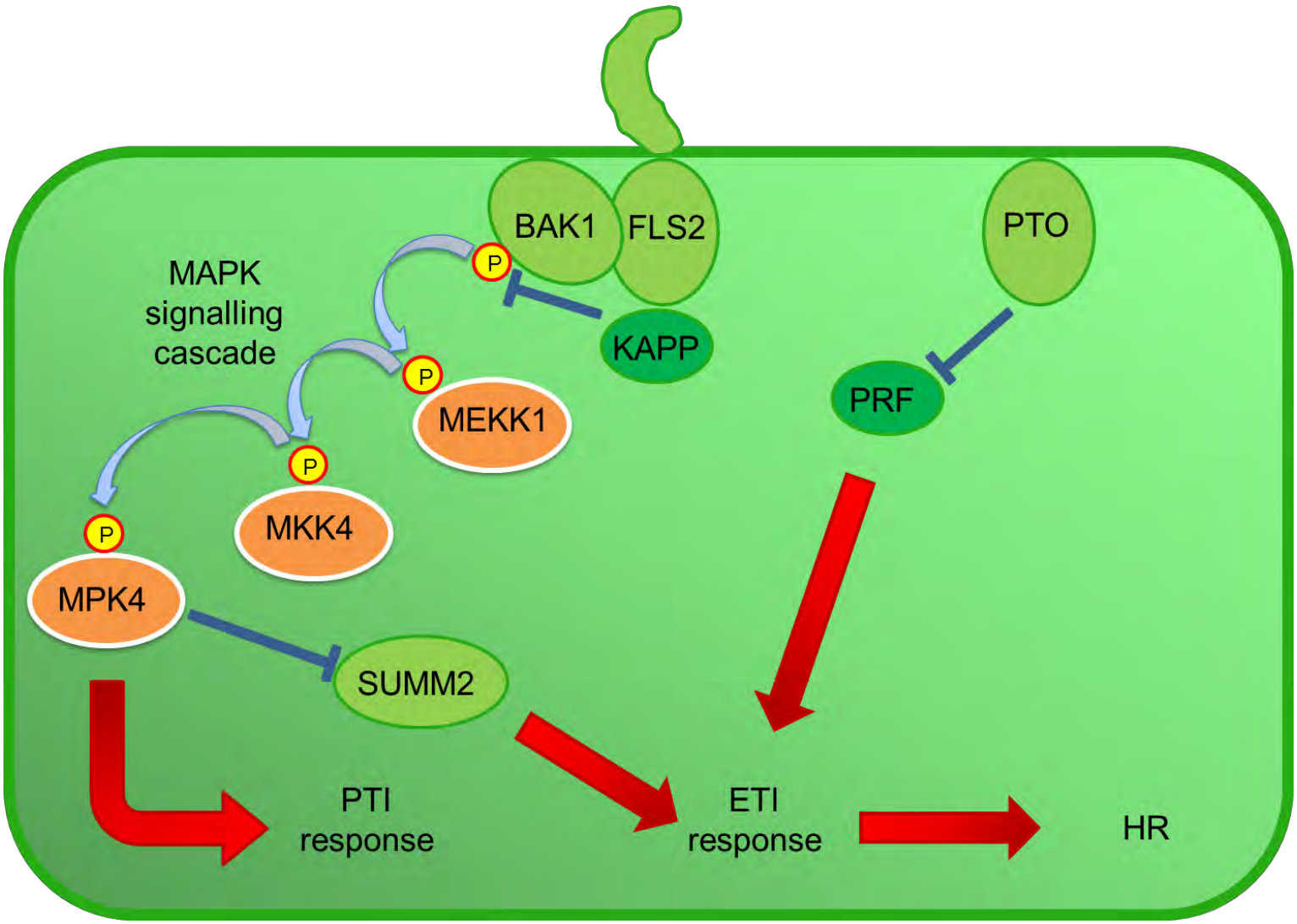

Figure 2| **Negative regulation of PAMP triggered immunity (PTI) and effector triggered immunity (ETI) in the absence of pathogen attack.** To prevent energetically expensive activation of defence responses in the absence of pathogen attack plants possess a number of negative regulators. The kinase-associated protein phosphatase (KAPP) directly inhibits autophosphorylation of the FLAGELLIN SENSING 2 (FLS2)/BRI1-ASSOCIATED RECEPTOR KINASE 1 (BAK1) heterodimer. This inhibits the sequential transfer of phosphate groups between mitogen-activated protein kinases (MAPKs) in the MAPK signalling cascade, and thus the induction of PTI is prevented. ETI activation by the resistance (R) protein PRF is prevented by constitutive interaction between PTO (serine/threonine kinase) and PRF. In the presence of pathogen associated molecular patterns (PAMPs), but not effectors, excessive activation of ETI is avoided though the suppression of the R protein SUMM2 by the MPK4 MAPK.

Environmental temperature affects plant defence

The effects of environmental temperature on plants are varied and depend, at least in part, on numerous other factors, including water availability, soil nutrients, and plant species (Garrett *et al*., 2006). As with plant growth and development, there are numerous examples of how temperature affects plant defence, with abnormally high or low temperatures during growth inhibiting disease resistance (Zhu, Qian & Hua, 2010). Heat sensitivity of *R* gene-mediated disease resistance has been observed in plants exposed to bacterial, fungal, and viral infection (Whitham, McCormick & Baker, 1996; Xiao *et al*., 2003; Wang *et al*., 2009), with disease resistance abolished above temperatures between 28^{o}C and 30^{o}C.

There are a number of mutants that display temperature dependent enhanced disease resistance; one such is *bonzai1* (*bon1*), a loss-of-function mutant that exhibits a constitutive defence response at 22^{o}C, but not at 28^{o}C (Yang & Hua, 2004). The *bon1* mutation leads to activation of *SUPPRESSOR OF NPR1-1, CONSTITUTIVE 1* (*SNC1*), an NB-LRR type *R* gene, resulting in downstream defence activation and SAR. The activation of *SNC1* and the consequent constitutive defence response, cause a dwarf phenotype in *bon1* at 22^{o}C; however, at 28^{o}C *SNC1* expression is suppressed, resulting in a loss of defence activation and no dwarf phenotype.

A *SNC1* gain-of-function mutant (*snc-1*) constitutively expresses *SNC1* and displays dwarfism, constitutive expression of defence genes and increased resistance to biotrophic pathogens. Like *bon1*, these phenotypes in *snc-1* are temperature dependant, with plants grown at 28^{o}C not displaying dwarfism or enhanced defence (Zhang *et al*., 2003).

Additionally, progeny of *bon1* and *snc1-11* (a null mutant) do not exhibit the *bon1* phenotypes, indicating that dwarfism and enhanced defence at 22^{o}C are SNC1 dependent.

Dwarfism and temperature dependent disease resistance in other mutants (*cpr1* and *srfr1*) have also been shown to be SNC1 dependent (Gou *et al*., 2009; Kim *et al*., 2010), suggesting that SNC1 may be a temperature sensor that modulates immunity in response to environmental changes. The *snc1-3* mutant (a constitutive expresser of *SNC1*) provides further evidence for this theory as it exhibits both dwarfism and enhanced resistance to virulent biotrophic pathogen *P. syringae* (*Pst* DC3000) at both 22^{o}C and 28^{o}C (Zhu, Qian & Hua, 2010). Interestingly, the fact that SNC1 nuclear content decreases with increasing temperature in wild type plants, but not in the *snc1-3* mutant could suggest that a threshold SNC1 concentration is required in the nucleus in order to trigger immunity.

The *cir1* mutant

Loss-of-function mutants that display constitutive expression of defence genes, like *bon1*, likely encode proteins that act as negative regulators of plant immunity. As discussed above, negative regulators occupy key positions in the plant defence signalling network, and enable tight regulation of defence gene expression(Trujillo *et al*., 2008), importantly preventing immune activation in the absence of pathogens. Therefore the identification of the *constitutively induced resistance 1* (*cir1*) mutant as a potential negative regulator of SAR (Murray *et al*., 2002) heralded a potentially interesting avenue for investigation.

The *cir1* mutant was identified following a mutant screen for increased luciferase activity in wild type *Arabidopsis thaliana* plants carrying a *PR-1:LUC* reporter construct. Increased

luciferase activity in the recessive *cir1* mutant compared to both wild type and *PR-1:LUC* lines indicated elevated activity of the *PR-1* promoter. Indeed, Northern blot analysis revealed the constitutive expression of a number of defence genes in *cir1*, including three *PR* genes, *PLANT DEFENSIN 1.2* (*PDF1.2*), and *GLUTATHIONE S-TRANSFERASE 1* (*GST1*) (Murray *et al*., 2002). Additionally, *cir1* shows enhanced resistance to infection by the virulent biotrophic pathogens *Pseudomonas syringae* (*Pst* DC3000) and *Hyaloperonospora arabidopsis*.

The *cir1* mutant shows enhanced resistance to infection by *Pst* DC3000 and to determine whether NPR1 is required for this defence phenotype, *cir1 npr1* double mutants were created. It was found that *npr1* reduced *PR-1* expression, suggesting that NPR1 is required for *cir1* mediated *PR-1* expression. Additionally, the *npr1* mutation was found to partially suppress disease resistance in the *cir1 npr1* double mutants suggesting that both *npr1*-dependent and -independent SA-mediated resistance contribute to disease resistance in *cir1* (Murray *et al*., 2002). The fact that the *cir1* null mutant displays constitutive expression of defence genes, and enhanced resistance to *Pst* DC3000, suggests that CIR1 is a likely negative regulator of plant defence.

Genetic mapping experiments and segregation analysis indicate that *cir1* is located on the lower arm of chromosome 4 of *A. thaliana* in a region containing 8 known genes (Carstens, 2008). Of these 8 genes, *AT4G11100* has been identified as the most likely candidate for *CIR1*; an *at4g11100* knockout line, containing a T-DNA insertion in the promoter region, displays elevated levels of PR-1 and EDS1 proteins, as well as enhanced resistance to infection by *Pst* DC3000 (Diener, 2012). AT4G11100 is a protein of unknown function that

has, interestingly, been shown to interact with two NB-LRR RLKs (AT2G36570 and AT3G50230) *in vitro* during yeast two hybrid assays (Mukhtar *et al*., 2011). Both RLKs appear to be involved in plant development, with evidence that AT2G36570 (P*XC PXY/TDR-CORRELATED GENE 1*, or *PXC1*) is important for secondary cell wall formation in xylem fibres (Wang *et al*., 2013). Although *in silico* analysis based on information from The *Arabidopsis* Information Resource (TAIR) broadly implicates *PXC* genes in defence and abiotic stress responses, Wang *et al.* (2013) found no clear link between *PXC1* and plant defence.

Project objectives

Relatively early in the course of the project it was discovered the *cir1* mutant displays a temperature sensitive growth phenotype. Since a number of other gain-of-resistance mutants display temperature dependant size and disease resistance, this novel finding prompted investigation into the effects of temperature on disease resistance in the *cir1* mutant.

The initial aim of the project was to confirm the role of *AT4G11100* as the gene responsible for the *cir1* disease resistance phenotype, as suggested by Diener (2012). This was to be done by characterising a second independent *AT4G11100* T-DNA insertion mutant, to ensure that the resistance phenotype displayed by the *AT4G11100* T-DNA insertion mutant previously characterised (Diener, 2012) was due to the disruption of *AT4G11100* and not due to multiple T-DNA insertions. While this second T-DNA insertion mutant did display the same phenotype as *cir1*, complementation of *cir1* and the *at4g11100* mutants showed that *AT4G11100* was not in fact *CIR1*, but was nonetheless a likely negative regulator of plant immunity. This hypothesis was tested by generating *AT4G11100* over-expressing transgenic

plants and analysing their resistance to *Pst* DC3000 and expression of several defence genes after infection. Finally, an attempt to determine the subcellular localisation of the AT4G11100 protein through the generation of eGFP-fusion proteins was undertaken.

Chapter 2: Methods and Materials

Plant Material and Growth Conditions

Plant lines

The wild type *Arabidopsis thaliana* seeds used in experiments were of the Columbia (Col-0) ecotype. The cir1 and PR1::LUC lines (in the Col-0 background) were obtained from Shane Murray (University of Cape Town). The T-DNA insertion lines SALK_062847C (promoter insertion) and SALK_096586 (exon 2 insertion) were obtained from the Nottingham Arabidopsis Stock Center (NASC) (Scholl, May & Ware, 2000).

Soil-grown plants

Seeds were hydrated in 0.1% (w/v) agar and left to stratify for 48 h at 4°C in the dark before being sown on a 1:1 mixture of peat (Jiffy Products, International AS, Norway) and vermiculite. Pots were covered with cling film to prevent soil desiccation and then placed at a constant temperature (22°C) under fluorescent light (100µM photons $m^{-2}s^{-1}$) with a 16 h light/ 8 h dark cycle. The cling film was removed after seven days; any excess seedlings were removed at the same time so that each pot contained only an individual plant.

Seed sterilization

Seeds sown on agar were sterilized in a lamina flow cabinet before plating. Seeds were placed in 1.5mL Eppendorf tubes and washed with 70% (v/v) ethanol for 5 min (tubes were inverted periodically). After washing, the 70% ethanol was poured off and replaced with 100% ethanol which was immediately aspirated. Seeds were allowed to dry on sterilized filter paper before being sown onto agar.

Agar-grown plants

Seeds were plated onto half strength Murashige and Skoog (MS) agar plates (8% w/v). MS agar pH was adjusted to 5.7 using 0.1M potassium hydroxide (KOH). Seeds were allowed to stratify on the plates for 48 h at 4°C in the dark, after which plates were placed at a constant temperature (22°C) under fluorescent light (100µM photons $m^{-2}s^{-1}$) with a 16h light/ 8h dark cycle.

Kanamycin selection

Plants expressing the kanamycin resistance gene (*NptII)* are resistant to the kanamycin antibiotic, and *NptII* homozygous lines (which display 100% resistance) can be selected for by growth on MS agar (0.8% w/v) containing 50mg/mL kanamycin. Between 1 and 2 weeks of growth, kanamycin sensitive plants can be distinguished from resistant individuals by their stunted leaf and root growth. Kanamycin resistant individuals were transferred to pots of soil and allowed to grow under normal soil growth conditions.

Microbial Strains and Plant Infection

Escherichia coli

E. coli strains DH5α and One Shot® (Life Technologies) were cultured in Luria-Bertani (LB) media (Sambrook *et al*, 1989) on either plates (1.5 % w/v agar) or in liquid culture, containing plasmid-dependent selective antibiotic(s). Bacteria were cultured at 37°C for 16 h overnight, with constant shaking (250rpm) for liquid cultures.

Agrobacterium tumefaciens

The *A. tumefaciens* strain GV3101 (Holsters *et al*, 1980) was cultured on LB agar plates (1.5% w/v agar) containing rifampicin (150 µg/mL) and gentamycin (15 µg/mL) at 28°C in the dark.

Pseudomonas syringae

The virulent strain *P. syringae* pv. *tomato* DC3000 (*Pst* DC3000) (Whalen *et al*., 1991) was cultured in King's Broth (KB) medium (King *et al*, 1954) on either plates (1.5 % w/v agar) or in liquid culture, containing 50 µg/mL rifampicin. Bacteria were cultured at 30°C for 16 h overnight, with constant shaking for liquid cultures.

***A. thaliana* infection assays**

Four week old soil grown *A. thaliana* plants were infected with a virulent *P. syringae* strain, *Pst* DC3000, according to the following protocol. A 5 mL overnight *P. syringae* culture was centrifuged and cells were then washed and resuspended in 10mM $MgCl_2$. Cells were diluted to give a final OD_{600} of 0.002, measured using the Beckman DU 650 Spectrophotometer (Beckman Coulter, Inc., CA, USA), in a total volume of 25mL. An OD_{600} of 0.002 corresponds to 1 x 10^6 colony forming units (c.f.u)/mL (Katagiri *et al*, 2002). Three leaves per plant were pressure infiltrated with the bacterial suspension using a needleless syringe. Five plants per plant line per time point (for harvesting at 4 or 48 h post infection) were infiltrated and an additional plant per line was infiltrated with 10mM $MgCl_2$ as a mock infection negative control. Infiltrated plants were covered with cling film and placed under normal growth conditions for 48 h. Infiltrated leaves were harvested at 4 h and 48 h post infection for bacterial growth analysis. Bacterial concentrations were determined by grinding three 0.5cm^2 leaf discs per plant (one for each infiltrated leaf) in 1mL 10mM $MgCl_2$

and making a serial dilution of the resulting bacterial suspension. Each dilution was then plated onto KB agar plates (50 µg/mL rifampicin) and incubated for 48 h at 30°C. Colony forming units were recorded for each sample and bacterial titre per cm^2 leaf area calculated.

DNA Manipulation

Isolation of genomic DNA from *A. thaliana*

A. thaliana genomic DNA was isolated from 100mg of leaf tissue per sample using a modified version of the Dellaporta (1983) DNA mini-preparation technique. The following modifications were made to the original protocol: Leaf tissue was not frozen with liquid nitrogen before being ground, but was homogenised directly in the extraction buffer.

Isolation of bacterial plasmid DNA

For moderate yields, bacterial plasmid DNA was isolated using the Wizard Plus DNA Purification System (Promega Corporation, Madison, US) according to the manufacturer's instructions. For larger yields, bacterial plasmid DNA was isolated using a modification of the DNA miniprep method used by Serghini *et al*. (1989). A single *E.coli* colony was inoculated into 5mL LB and incubated for 16 h overnight, after which 1.5mL samples of culture were centrifuged at 13 000 rpm in 1.5mL Eppendorf tubes for 45 s. After centrifugation the supernatant was discarded and 50µl of a TEN buffer (10mM Tris-HCl, pH 8.0, 1mM EDTA, 100mM NaCl) was added to each sample. Cells were resuspended by vortexing for 2 min and 50µl of a phenol/chloroform/isoamyl alcohol mixture (25:24:1 v/v) was added. Following a brief mix by vortexing, samples were centrifuged at 13 000 rpm for 5 min, and the supernatant transferred to a new 1.5mL Eppendorf tube containing 100µl isopropanol.

After the transfer, 17µl of 7.5M ammonium acetate (NH_4OAc) was added to samples, which were briefly mixed before being centrifuged at 13 000 rpm for 1 minute. After centrifugation the supernatant was discarded and the pellet rinsed with 70% (v/v) EtOH. Samples were aspirated and the DNA resuspended in 40µl H_2O.

DNA amplification

DNA was amplified using Supertherm DNA Polymerase (Separations Scientific SA Pty Ltd., Honeydew, South Africa) in a polymerase chain reaction (PCR). Table 1 describes the PCR primers used in experiments, their sequence information, and annealing temperatures (T_A). Each reaction had a total volume of 20µl and included 1.5mM $MgCl_2$, 1 x PCR Buffer, 0.4µM of each primer, 0.2mM dNTPs (Fermentas, Ontario, Canada), 0.5U Supertherm DNA Taq polymerase. Typically between 100 – 200ng template DNA was used in each reaction. The following cycling conditions were used for all reactions: Initial denaturation at 94°C for 5 min followed by 35 cycles (94°C for 15 s, T_A for 30 s, and 72°C for 15 s/kilobase of product) and a final elongation at 72°C for 10 min. All PCR reactions were carried out in a Gene Amp PCR System 2700 (Applied Biosystems, Foster City, USA).

High fidelity PCR

When cloning, a high fidelity Velocity DNA polymerase (Bioline Ltd., London, UK) was used in PCR reactions to reduce the polymerase error rate. Reactions were prepared according to the manufacturer's protocol using the following cycling conditions: Initial denaturation at 98°C for 2 min followed by 35 cycles (98°C for 30 s, T_A for 30 s, and 72°C for 30 s/kilobase of product) and a final elongation at 72°C for 10 min.

Table 1| **PCR primers used during the course of this project.**

Primer name	**Sequence**	**Annealing Temp (^{o}C)**
Cloning		
AT4G11100 – F	AGGATCCATGATGTTTGGTTTAGAGAAAACG	55
AT4G11100 – R	AGAATTCAGAGGCTTGTTGGAATCCTTCC	55
AT4G11100stop – R	AGAATTCCTAAGGCTTGTTGGAATCC	55
Genotyping		
At-LP	AAACGATGACTTTGGAGCATG	55
At-RP	AACTCCTGACAAAAACAGAAAGC	55
LBb1.3	ATTTTGCCGATTTCGGAAC	55
Sequencing		
GFP fusion	AGATGAACTTCAGGGTCAG	50

DNA electrophoresis

Electrophoresis of DNA was performed using a 1% (w/v) agarose gel containing 0.016µg/mL ethidium bromide (EtBr). Gels were prepared using 1 x TAE buffer (40mM Tris, 1mM EDTA, 0.11% (v/v) glacial acetic acid). DNA was separated alongside a 1 Kb size marker (O' Gene Ruler ™ DNA ladder, Fermentas, Ontario, Canada). All gels were electrophoresed in 1 x TAE buffer for approximately 1 h, after which DNA was visualised with a long wavelength (365 nm) UV transilluminator.

Gel extraction of DNA

DNA was purified from the gel slice using the Wizard SV Gel and PCR Clean up system (Promega Corporation, Madison, USA) according to the manufacturer's protocol.

Restriction endonuclease digestion of DNA

Fermentas International Inc. (Ontario, Canada) restriction enzymes (REs) were used in the digestion of plasmid or purified PCR DNA. Reactions typically required between 5 -10 Units of RE, and were carried out according to the manufacturers recommended conditions.

Ligation of DNA

Ligation reactions consisted of purified insert and vector DNA, 3 – 5 Units of T4 DNA Ligase (Fermentas lnternational Inc., Ontario, Canada), and 1 x T4 DNA Ligase buffer. A vector:insert ratio of 1:3 was used in all ligation reactions, with the amount of insert required (ng) calculated using the following equation:

$$\frac{\text{quantity of vector DNA (ng)} \ \text{x} \ \text{size of insert DNA (Kb)}}{\text{size of vector DNA (Kb)}} \ \text{x} \ \text{insert: vector molar ratio}$$

Reactions were performed according to the manufacturer's protocol and incubated overnight at 4 °C.

LR Gateway cloning

Gateway cloning utilizes *att*L- and *att*R- sites to facilitate the transfer of a desired fragment of DNA from an entry vector to a destination vector. The transfer of a DNA fragment from

between the *att*L- sites of the entry vector to between the *att*R- sites of the destination vector is performed through LR recombination. LR recombination was performed according to the manufacturer's protocol.

Entry Vector

pENTR™4 Dual selection vector

This vector contains a *ccdB/chloramphenicol* fusion gene between the *att*L- and *att*R- sites which allows for negative selection of DH5α *E.coli* cells that are sensitive to the ccdB protein. The empty vector was propagated in One Shot® *ccdB* Survival™2 T1R *E.coli* cells that are ccdB insensitive, in the presence of 50 µg/mL kanamycin, which was also used to select for positive DH5α transformants.

Destination Vectors

pFAST-G02

This vector contains a *ccdB* gene between the *att*L- and *att*R- sites which allows for negative selection of DH5α *E.coli* cells that are sensitive to the ccdB protein. The empty vector was propagated in One Shot® *ccdB* Survival™2 T1R *E.coli* cells that are ccdB insensitive, using either 50 µg/mL spectinomycin or 50 µg/mL streptomycin to select for positive trasformants. pFAST-G02 contains the herbicide resistance gene *Bar*, which allows for the identification of transformed plants via phosphinothricin selection. Alternatively, transformed plant seeds can be identified under a fluorescent microscope as they express enhanced green fluorescent protein (EGFP).

pK7FWG2.0

This vector contains a *ccdB/chloramphenicol* fusion gene between the *att*L- and *att*R- sites which allows for negative selection of DH5α *E.coli* cells that are sensitive to the ccdB protein. The empty vector was propagated in One Shot® *ccdB* Survival™2 T1R *E.coli* cells that are ccdB insensitive, using 50 µg/mL spectinomycin, 50 µg/mL streptomycin, or 50 µg/mL kanamycin to select for positive trasformants. pK7FWG2.0 contains an *EGFP* gene immediately following the *att*R2 site, which is designed to translationally fuse with genes transferred through LR recombination.

***E. coli* competent cell preparation**

A single *E.coli* colony was inoculated into 5mL LB media and grown for 16 h overnight. Two mL of the overnight culture were added to 250mL LB media containing 20mM $MgSO_4$, which was left to grow at 37°C while shaking until the OD_{600} was between 0.4 and 0.6. The culture was then centrifuged in in a JA-21 Beckman centrifuge at 5000 x g for 5 min at 4°C and the supernatant discarded. Cells were resuspended in 100mL ice cold TFB1 (a filter sterilized buffer containing 30mM KAc, 100mM RbCl, 10mM $CaCl_2$, 50mM $MnCl_2$, 15% glycerol (v/v), adjusted to pH 5.8 using glacial acetic acid) and kept on ice for 5 min. The suspension again centrifuged at 5000 x g for 5 min at 4°C and the supernatant discarded. The pellet was resuspended in 10mL ice cold TFB2 (a filter sterilized buffer containing 10mM MOPS, 75mM $CaCl_2$, 10mM RbCl and 15% glycerol (v/v)) and kept on ice for between 15 and 60 min. Competent cells were divided into pre-cooled 1.5mL Eppendorf tubes in 100µL aliquots, and frozen immediately in liquid nitrogen. Cells were stored at -80°C.

Transformation of competent *E.coli* cells

Between 50 and 100ng of plasmid DNA were added to 100 µl ice-thawed competent *E. coli* cells. After the addition of the DNA, cells were left on ice for 30 min, followed by a heat shock at 42°C for 45 s and then snap cooled on ice for 2 min. Nine hundred µL of LB media was added and cells were incubated at 37°C for 60 min with shaking. Following incubation, 100µl of each culture was plated on LB plates (1.5 % w/v agar) with the appropriate antibiotics before being incubated at 37°C for 16 h overnight.

Glycerol stocks

Glycerol stocks of positive transformed cells lines containing a vector of interest were created for storage. Glycerol stocks were created by adding 680µL of freshly grown overnight culture to 320µL of pre-sterilized 50 % glycerol in a 1.5 mL Eppendorf. Stocks were flash frozen in liquid nitrogen and stored at -80°C.

DNA sequencing and analysis

All DNA sequencing was performed at the Central Analytical Facility (Stellenbosch, South Africa) on an ABI3730xl DNA analyser (Applied Biosystems, Foster City, USA). Sequence data was analysed using Chromas software (Version 2.01, Technelysium Pty Ltd, Queensland, Australia) and BLAST (http://blast.ncbi.nlm.nih.gov/Blast.cgi).

RNA Manipulation

Isolation of RNA from *A. thaliana*

Total RNA was extracted using a TRIzol reagent (100mM NaAc pH 5.2, 800mM guanidine thiocyanate, 400mM ammonium thiocyanate, 5% glycerol (v/v) and 38% phenol (v/v) pH 4, made up in DEPC-treated dH_2O) based on the Chomczynski & Mackey (1995) RNA extraction protocol. RNA was extracted according to the TRIzol reagent protocol (Invitrogen, Carlsbad, USA) with the following modification: Plant tissue was homogenised in 1.5mL Eppendorf tubes each containing 3 stainless steel ball bearings and 1mL TRIzol reagent. Tubes were subjected to 4 min of mechanical shaking in a paint shaker.

Electrophoresis of RNA

Electrophoresis of RNA was performed using a RNA formaldehyde-agarose denaturing gel, containing 1 x MOPS pH 7 (0.4M MOPS, 0.1M NaAc, 10mM EDTA), 1.2% (w/v) agarose, and 2.25% (v/v) formaldehyde. Prior to electrophoresis, RNA samples were mixed with 0.2 volumes of RNA sample application buffer (4 x MOPS, 2.7% (v/v) formaldehyde, 30.8% (v/v) formamide and 0.01 mg/mL EtBr), heated at 65°C for 5 min and snap cooled on ice. RNA was visualised on a Gel Doc™ XR UV transilluminator (Bio-Rad Laboratories, UK).

DNase treatment of RNA

RNA to be used in cDNA synthesis was first treated with DNAse from the Turbo DNA-free™ kit (Life Technologies, California, USA) as instructed by the manufacturer.

cDNA synthesis

cDNA synthesis was performed using Superscript III Reverse Transcriptase (Life Technologies, California, USA) according to the manufacturer's protocol with the following modifications: 2.5µg total RNA and half volume of the Superscript™ III enzyme were used; cDNA synthesis was performed at 42°C for 2 h, followed by a heat inactivation step at 72°C for 15 min.

Quantitative real-time PCR (qPCR)

All qPCR reactions were performed using the KAPA SYBR® FAST qPCR Kit, according to the manufacturer's protocol. A Rotor-Gene® 6000 Real-Time PCR machine (QIAGEN, Limburg, Netherlands) was used to amplify cDNA under the following cycling conditions: 95°C for 3 min, followed by 40 cycles (95°C for 3 s, 60°C for 20 s, and 72°C for 1 s), and a final step at 72-95°C for 5 min. Rotor-Gene® Series Software (version 1.7) was used for melt curve analysis and quality control (with a minimum R^2 value of 0.99, slope values between 3.3 and 3.5 required for a run to be considered "good"; slope values near 3.3 reflect a reaction efficiency of near 100%). Table 2 details all primers used for qPCR experiments in this project, their sequences, and the concentrations at which they were effective.

Table 2| **qPCR primers used during the course of this project.**

Gene name	Locus	Primer pair sequences	Final concentration (nM)
ACT2	AT3G18780	AGTGGTCGTACAACCGGTATTGT	900
		CATGAGGTAATCAGTAAGGTCACGT	300
SNC1	AT4G16890	GCTCGCCGACTTTACAGACT	200
		GGAAGATGATACAACTTATCCCAGA	200
AT4G11100	AT4G11100	GTAGTAGCTTCGGTTACTCAAAGT	200
		GCATCTGTCACAGCATTGTTC	200
PR2	AT3G57260	TCTTCAACCACACAGCTGGA	200
		TCTGAACTGGGAACGTCGAG	200
ICS1	AT1G74710	GCTAGCACAGTTACAGCGTG	200
		AAGCTTCACTGCAGACACCT	200

Western Blots

Crude protein extraction from *A. thaliana*

A. thaliana leaf tissue was homogenised in an extraction buffer (10mM Potassium Phosphate pH7.2, 5mM DTT) and centrifuged for 5 min at 10 000 rpm. Protein concentrations of extracts were determined though a Bradford assay.

SDS Polyacrylamide Gel preparation

A 15% polyacrylamide gel was prepared and electrophoresed using a Mini-PROREAN® 3 system (BioRad Laboratories, Inc. Hercules, USA). In all gels a 40% (w/v) Acrylogel acrylamide/bisacrylamide (29:1 v/v) stock solution (Sigma-Aldrich Inc., St Louis, USA) was utilized. A resolving gel (20% (v/v) Acrylogel, 375mM Tris-HCl ph8.8, 0.2% (w/v) SDS, 0.1%

(w/v) APS, 0.1% (v/v) TEMED) was overlaid by a stacking gel (4% (v/v) Acrylogel, 125mM Tris-HCl pH6.8, 0.1% (w/v) SDS, 0.09% (w/v) APS, 0.1% (v/v) TEMED).

SDS Polyacrylamide Gel Electrophoresis (SDS-PAGE)

Heat denatured crude protein samples, together with 1x loading buffer, and a molecular weight marker (PageRuler™ Prestained Protein Ladder; Fermentas lnternational Inc., Ontario, Canada) were loaded onto the polyacrylamide gel. Samples were electrophoresed in a running buffer (25mM Tris-HCl pH8.8, 192mM glycine and 0.1% (w/v) SDS) for 30 min at 60 volts, as they moved through the stacking gel. The voltage was then increased to 200 volts until the dye front had run off the bottom of the resolving gel.

Protein transfer

Protein samples were transferred from the polyacrylamide gel onto a nitrocellulose membrane (Schleicher and Schuell BioScience, Dassal, Germany) for 1 hour at 15 volts, using the Biorad semi-dry transblotter apparatus (BioRad Laboratories, Inc. Hercules, USA) as per manufacturer's instructions. The membrane and blotting paper were pre-soaked in transfer buffer (25mM Tris, 192mM glycine and 20% (v/v) methanol).

Blocking and eGFP incubation conditions

Nitrocellulose membranes with transferred protein were blocked with blocking buffer (1 x PBS(58mM $Na_2HPO_4.2H_2O$, 18mM KH2PO4, 1.37M NaCl, 26mM KCl), 5% milk powder (w/v), 0.1% (v/v) Tween) for 30 min at 22°C with shaking. Roche mouse anti-GFP antibodies were used to detect the presence of eGFP in protein samples.

A. thaliana **transformation**

Plant preparation

Soil grown plants were allowed to grow for 4 weeks until the first inflorescence shoot began to appear. These inflorescence shoots were removed as this encourages growth of multiple secondary inflorescences. The next inflorescence shoots were again removed, after which the plants were allowed to grow until a large number of unopened flower heads appeared.

A. tumefaciens competent cell preparation

A 10 mL LB medium, supplemented with the appropriate antibiotics, was inoculated with a single colony of *A. tumefaciens* and incubated at 28°C for 16 h overnight with shaking. 2 mL of this culture was transferred to 50 mL fresh LB media (with appropriate antibiotics) and incubated with shaking at 28°C until the OD600 reached 0.5–1.0. The culture was chilled on ice before the cells were harvested by centrifugation at 3000 x *g* for 5 min at 4°C in a J2-21 Beckman centrifuge (Beckman Coulter, Inc., CA, USA). Pelleted cells were resuspended in 1 mL ice cold 20 mM CaCl2. Aliquots of 100µl were then immediately frozen in liquid nitrogen and stored at -80°C.

Transformation of competent *A. tumefaciens*

The 100µl competent *A. tumefaciens* cell aliquots were defrosted on ice for approximately 5 min. After the cells had defrosted, between 50 and 100ng of plasmid DNA was added to the Eppendorf tube. Following the addition of the DNA, cells were heat shocked at 37°C for 5 min. Nine hundred µL of LB media were added and cells were incubated at 30°C for 6 h while shaking. Following incubation, 100µl of each culture was plated on LB plates (1.5 %

w/v agar) with the appropriate antibiotics before being incubated at 30°C for between 2 and 3 days.

Floral dip transformation of *A. thaliana*

A. thaliana plants were transformed following a protocol based on the floral dip method used by Clough and Bent (1998). Any open flower heads were removed before submerging the aerial parts of plants in an *A. tumefaciens* suspension for 5 s. Dipped plants were left on their sides in a paper towel-lined tray which was then covered with clingfilm and left for 16 h overnight at 22°C. Plants were then placed upright in a tray and allowed to grow normally until siliques were fully formed, after which the plants were allowed to dry for seed collection.

Herbicide selection of plants containing *pFAST-G02*

Transgenic plants expressing the *Bar* gene are resistant to herbicides containing glufosinate ammonium (phosphinothricin), which can be used to select for *Bar* containing plants (homozygous plants will display 100% resistance). After 5 days of growth, soil grown transgenic plants were sprayed with a 0.015% (w/v) Basta solution (Basta is a herbicide containing glufosinate ammonium) so that all leaf surfaces were damp. Two more rounds of herbicide spraying took place at 8 and 11 days of growth, after which resistant plants could be distinguished by healthy green leaves, and sensitive plants by pale yellow leaves.

A. thaliana protoplast isolation and transfection

A. thaliana protoplasts were isolated and transfected with plasmid DNA according to the method used by Yoo *et al.* (2007)**.** A Zeiss LSM 510 Meta confocal microscope was used for imaging transfected protoplasts, utilizing a LD C-Apochromat 403/1.1 W M27 objective. Excitation of GFP was performed at 488 nm and emission detected in the 500 to 520 nm range.

Luciferase assays

Luciferase activity was detected using the Luciferase Assay System (Promega Corporation, Madison, US) according to the manufacturer's instructions, utilizing a Modulus microplate luminometer.

Data analysis

All data analysis was performed using StatSoft Statistica software. Fisher LSD post hoc tests were used in the Analysis of Variance (ANOVA) tests of differences between groups.

Chapter 3: Results and Discussion

The *cir1* growth and disease resistance phenotypes are temperature dependent

Environmental temperature modulates both growth and disease resistance in wild type plants (Garrett *et al*., 2006); with higher growth temperatures often associated with compromised immunity and greater plant growth. Similarly, in a number of gain-of-resistance mutants, including *constitutive expressor of PR genes 1* (*cpr1*), *suppressor of rps4-RLD 1* (*srfr1*), *bonzai1* (*bon1*), and *suppressor of npr1-1, constitutive 1* (*snc-1*), enhanced resistance to pathogen attack and constitutive expression of defence genes are abolished when these plants are grown at higher temperatures (Zhang *et al*., 2003; Gou *et al*., 2009; Kim *et al*., 2010). The *constitutively induced resistance 1* (*cir1*) mutant is also a constitutive expresser of a number of plant defence genes, including *PATHOGENESIS RELATED-1* (*PR-1*), and displays enhanced resistance to infection by virulent bacterial pathogens including *Pseudomonas syringae* (Murray *et al*., 2002), but whether these phenotypes are similarly modulated by environmental temperature is unknown.

The effects of temperature on the growth of the *cir1* mutant were investigated by growing *cir1* and *PR-1:LUC* (*cir1* genetic background) plants at 18^{o}C, 22^{o}C (standard growth temperature), and 25^{o}C for 4 weeks (Figure 3). Temperature clearly influenced plant growth in both lines, with much smaller plants observed at 18^{o}C and progressively larger individuals at 22^{o}C and 25^{o}C respectively. A marked difference in the size of *cir1* and *PR-1:LUC* plants was observed at 18^{o}C, with *cir1* individuals growing considerably smaller than *PR-1:LUC* individuals. This size difference was less obvious at 22^{o}C, and was completely absent at 25^{o}C.

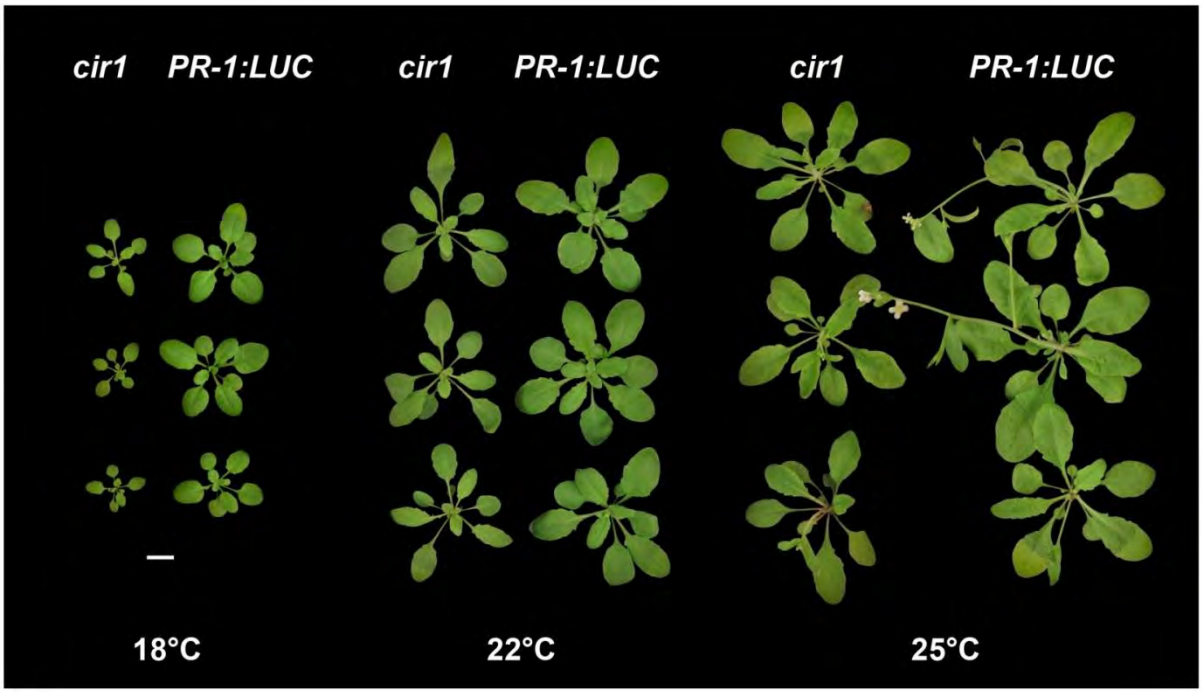

Figure 3| **Temperature sensitive growth phenotype of *cir1*.** The *cir1* mutants displays reduced growth at 18°C as compared to *PR-1:LUC* control plants. Plants were grown for four weeks under a 16 hour light/8 hour dark cycle at 18°C, 22°C or 25°C. Scale bar represents 10mm.

Thus, like other gain-of-resistance mutants, *cir1* displays a temperature dependent growth phenotype. However, *cpr1, srfr1, bon1, and snc-1* all display a temperature modulated growth phenotype where plants are dwarfed at temperatures between 22^{o}C and 28^{o}C (Zhang *et al*., 2003; Gou *et al*., 2009; Kim *et al*., 2010). The *cir1* mutant clearly differs from these mutants as it only exhibits reduced growth at 18^{o}C, which is completely abolished at 22^{o}C.

To determine whether the enhanced resistance to infection by *P. syringae* displayed by *cir1* under normal growth conditions (22^{o}C), is also modulated by temperature, 4 week old *cir1* and *PR-1:LUC* plants grown at 18^{o}C, 22^{o}C, and 25^{o}C were infected with a virulent *P. syringae* pv. *tomato* DC3000 (*Pst* DC3000) strain, and bacterial growth quantified 48 h post infection

(Figure 4). The *cir1* mutant shows significantly lower bacterial titres when compared to *PR-1:LUC* at both 18^{o}C ($p < 0.05$) and 22^{o}C ($p < 0.05$), but not at 25^{o}C. Interestingly, the fold difference in bacterial titre 48 h post infection between *cir1* and *PR-1:LUC* is greater at 18^{o}C (29 fold) than at 22^{o}C (7 fold) and bacterial titres in the *cir1* mutant are significantly lower at 18^{o}C versus 22^{o}C (Figure 4). This demonstrates that there is an increased defence response in *cir1* at 18^{o}C that gradually lessens as growth temperature increases, and is abolished at 25^{o}C. Taken together, the reduced growth and increased resistance to *Pst* DC3000 of *cir1* at 18^{o}C suggests that these are temperature dependent characteristics (i.e. enhanced resistance is lost at higher temperatures) and that there is likely an energetic cost associated with the constitutive expression of defence genes in *cir1* which results in reduced biomass production at 18^{o}C.

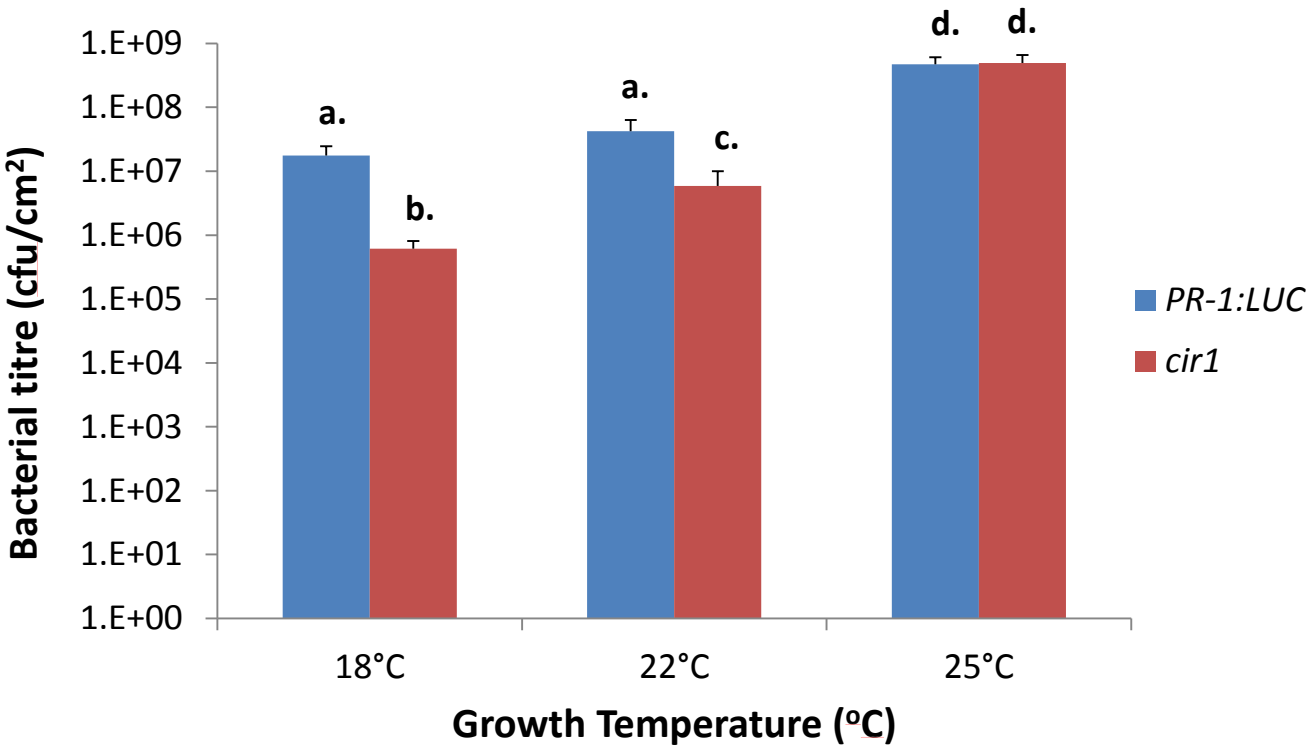

Figure 4| **Temperature sensitive pathogen resistance phenotype of *cir1*.** Mean *P. syringae* titre (+SE, n = 5) 48 h post infection in *cir1* and *PR-1:LUC* control lines. Plants were grown for four weeks at 18°C, 22°C and 25°C prior to infection with *Pst* DC3000. Letters indicate significant differences ($p < 0.05$) determined by ANOVA with Fisher LSD. This experiment is representative of three independent experiments.

The temperature conditional phenotype of *cir1* could explain the "variable nature of the *cir1* mutant" described in previous work (Carstens, 2008; Diener, 2012). This variability refers to several instances where the bacterial titres in *cir1* plants did not significantly differ from those of control lines during pathogen assays performed on plants grown in the departmental plant growth room, which is subject to temperature fluctuations several degrees above 22. In contrast, the experiments described above were carried out in Perceval growth chambers where the temperature is more reliably kept constant through a computer controlled temperature regulator. Given what is now known about the

temperature sensitivity of the *cir1* mutant, the instances where *cir1* displayed a "variable nature" may well have been the result of fluctuating temperatures during growth leading to the repression of the *cir1* phenotype.

The nucleotide-binding and leucine-rich repeat (NB-LRR) R protein, SNC1, is essential for the dwarfed growth and constitutive defence gene expression in the gain-of-resistance mutants *bon1*, *cpr1*, and *srfr1*, which display elevated *SNC1* RNA and/or protein levels (Yang & Hua, 2004; Gou *et al*., 2009; Kim *et al*., 2010). It is possible SNC1 acts as a temperature sensor that modulates plant immunity in response to changes in environmental temperature, and may do this once a threshold amount of SNC1 has localised in the nucleus (Zhu, Qian & Hua, 2010). To investigate whether SNC1 might be similarly important to the growth and resistance phenotypes in *cir1*, *SNC1* expression was analysed in *cir1* and *PR-1:LUC* plants grown at 18^{o}C and 22^{o}C (Figure 5). However, quantitative real-time PCR (qPCR) analysis of *SNC1* mRNA from 4 week old plants revealed no significant differences in *SNC1* transcript levels between *cir1* and *PR-1:LUC*, at either 18^{o}C or 22^{o}C, suggesting that the *cir1* phenotypes may be independent of SNC1 mRNA levels. In order to definitively determine whether or not SNC1 is required for the defence phenotype of *cir1*, a cross between the *cir1* mutant and a *snc1* knockout mutant would need to be performed. If the offspring of such a cross continued to display enhanced disease resistance, this would indicate that the *cir1* defence phenotype is indeed SNC1 independent.

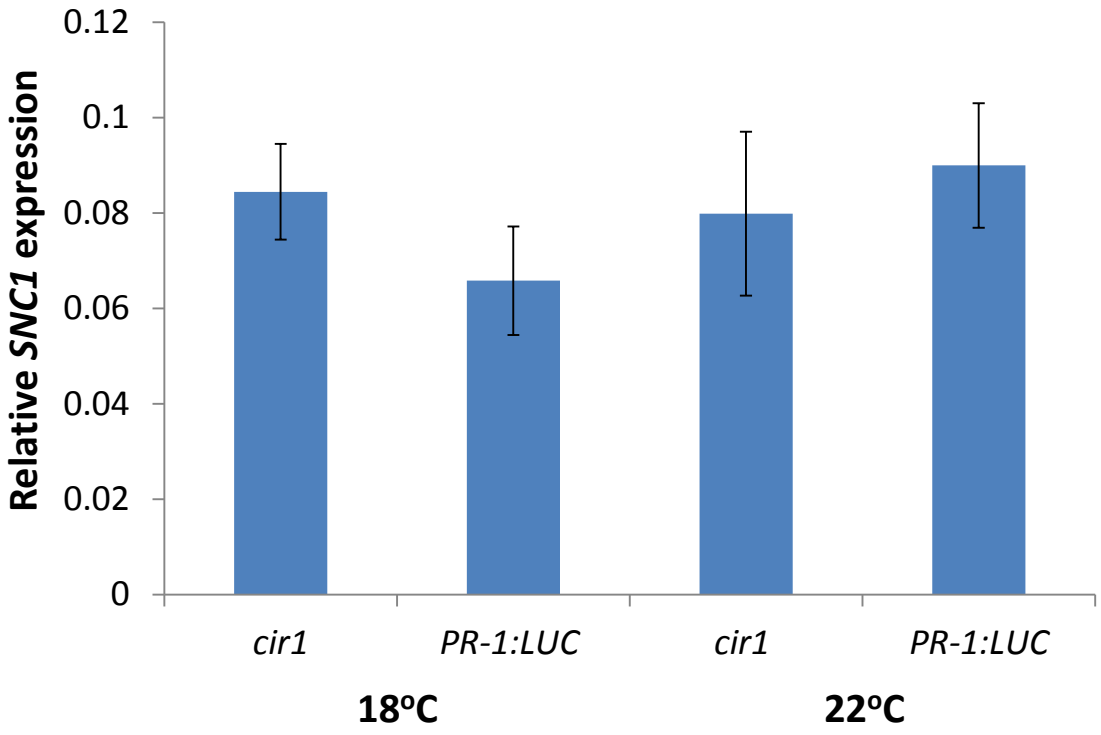

Figure 5| **Relative *SNC-1* mRNA levels in *cir1* and *PR-1:LUC* plants at 18°C and 22°C.** mRNA levels were normalised against *ACTIN*-2. Plants were grown for four weeks under a 16 hour light/8 hour dark cycle at 18°C or 22°C.

Identification and characterisation of a second *at4g11100* T-DNA insertion mutant

The *cir1* mutant was originally identified and characterised by Murray and colleagues (2002); subsequent work has involved attempts to identify the gene responsible for the *cir1* phenotype. Through a series of genetic mapping experiments, the location of the *CIR1* gene was narrowed down to a region of chromosome IV, where 8 possible gene candidates are present (Carstens, 2008). Homozygous T-DNA insertion mutants for each of the 8 candidate genes were obtained and analysed in order to determine if any phenocopied *cir1*. Unlike the other seven mutants, the *at4g11100-p* mutant (SALK_062847 - containing a T-DNA insertion in the promoter region of the *AT4G11100* gene) displayed elevated levels of PR-1 protein

and was found to be more resistant to infection by *Pst* DC3000 as compared to wild type *A. thaliana*; for this reason *AT4G11100* was considered to be the most likely candidate for the *CIR1* gene (Diener, 2012).

In the present study, to ensure that the phenotype of the *at4g11100-p* mutant was indeed due to a disruption of that gene and not an artefact of multiple T-DNA insertions in this plant line, a second *at4g11100* T-DNA insertion mutant was obtained - *at4g11100-e* (SALK_096586 - containing a T-DNA insertion in exon 2). However, a homozygous *at4g11100-e* line was unavailable and so it was necessary to screen a segregating line to identify homozygous individuals. Screening was undertaken using a PCR based method that utilized either *AT4G11100* gene-specific primers, or T-DNA insert-specific primers (Figure 6A). The *AT4G11100* gene-specific primers (At-LP and At-RP) were designed in positions flanking the predicted site of T-DNA insertion, and because the insert is almost 5kb in size, amplification using the gene-specific primers is impossible in the presence of the insert; similarly, the T-DNA insert-specific primers (At-RP and LBb 1.3) generate a PCR product only in the presence of the insert. Therefore, using these two primer pairs it is possible to determine if an individual plant is homozygous for either the wild type or T-DNA insertion *at4g11100* alleles, or if an individual is a heterozygote containing both alleles (Figure 6B). Once homozygous *at4g11100-e* plants were identified, they were separated from the others and allowed to set seed; homozygous *at4g11100-e* seed stocks were generated in this way.

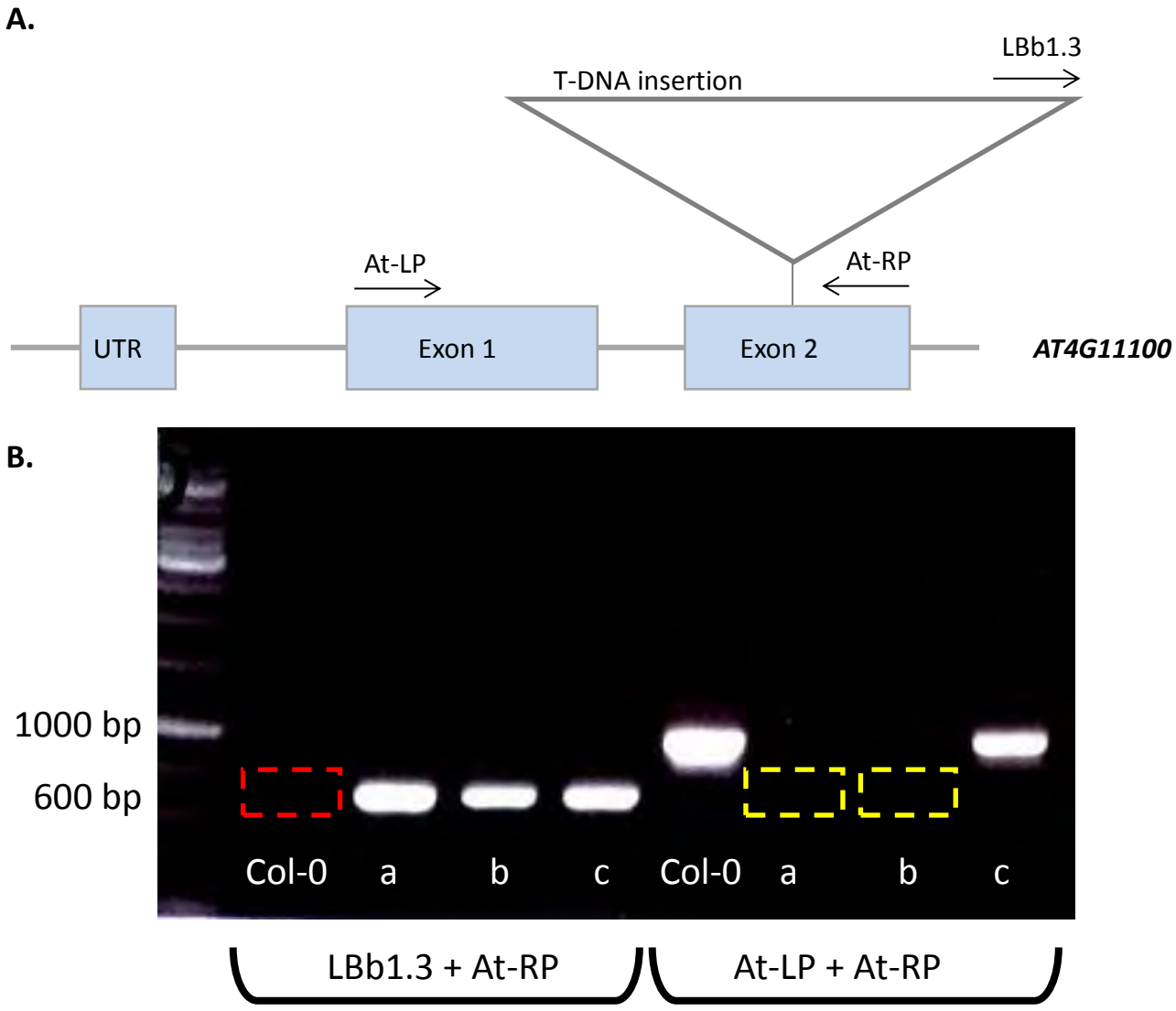

Figure 6| ***at4g11100-e* T-DNA insert position and identification of a homozygous T-DNA insertion line.** A) The At-LP and At-RP gene-specific primers are designed to amplify wild type *AT4G11100* and flank the predicted site of T-DNA insertion. The LBb1.3 insert-specific primer is located on the border of the T-DNA insert and generates a product with At-RP only in the presence of a T-DNA insertion. Exons are indicated by boxes, while primers and the direction of their amplification are indicated by arrows. B) PCR amplification of genomic DNA extracted from a wild type Columbia (Col-0) plant and three plants (a, b, and c) from the *at4g11100-e* T-DNA insertion line. DNA was amplified using either T-DNA insertion specific primers (LBb1.3 + At-RP) or wild type *AT4G11100* primers (At-LP + At-RP). The red box highlights the lack of amplification of Col-0 DNA when using T-DNA insertion specific primers. The yellow boxes highlight the lack of amplification of DNA from plants a and b using wild type *AT4G11100* primers. Plants a and b are homozygous for the T-DNA insertion. Plant c is heterozygous for the insertion.

Additionally, the PCR product obtained with the LBb1.3 and At-RP primers was sequenced to determine the exact site of T-DNA insertion. The predicted site of T-DNA insertion in *at4g11100-e* according to The *Arabidopsis* Information Resource (TAIR) is 814bp downstream of the ATG start codon, in exon 2; however, sequencing data revealed that the actual site of insertion is approximately 250bp further upstream, at 563bp downstream of the ATG start codon, in the middle of an intron (Figure 7).

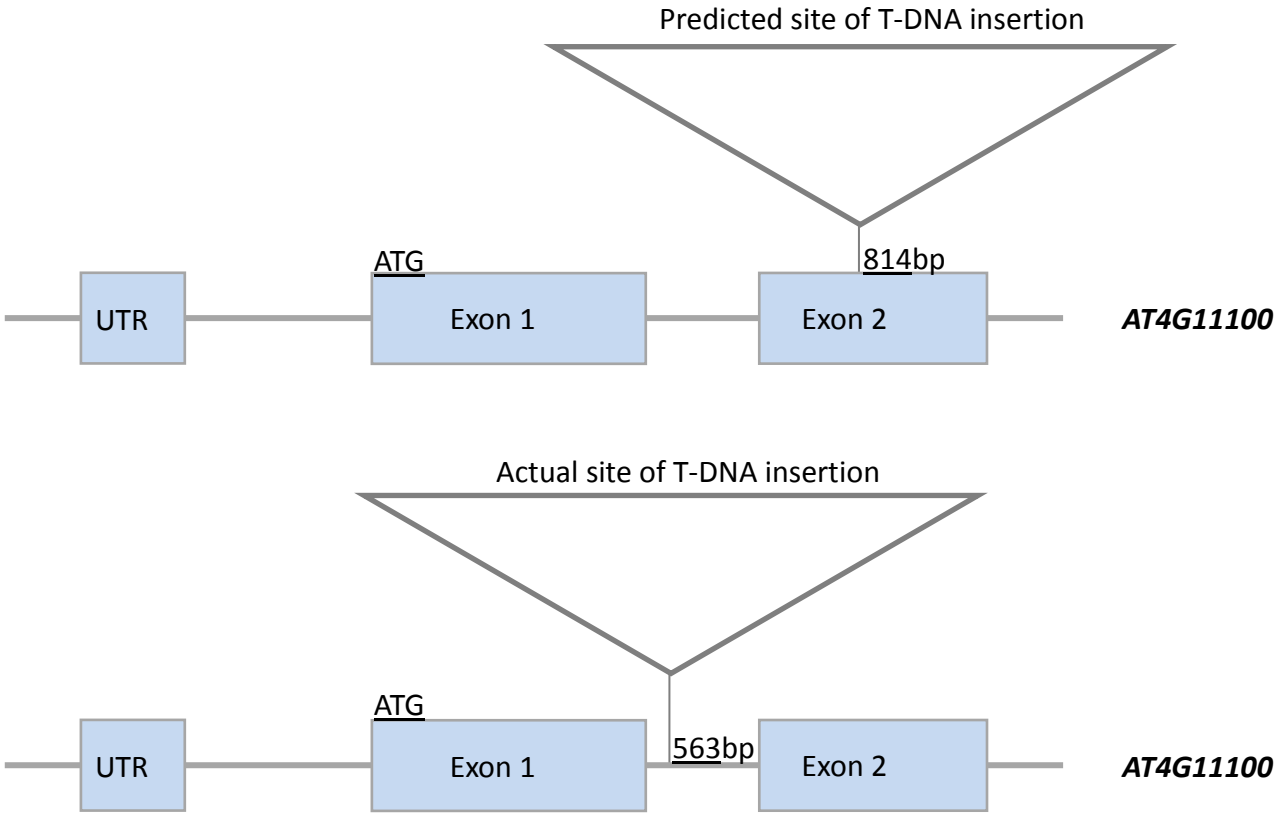

Figure 7| **Predicted and actual position of T-DNA insertion in *at4g11100-e*.** The predicted site of T-DNA insertion in *at4g11100-e*, according to The *Arabisopsis* Information Resource (TAIR – arabidopsis.org), is 814bp downstream of the ATG start codon. Sequencing data shows the actual site of T-DNA insertion in *at4g11100-e* is 563bp downstream of the ATG start codon.

It is also necessary to determine that T-DNA insertion lines are true knock-outs for the gene of interest, especially given the fact that the T-DNA insert in this line is in an intron. To this end, reverse transcriptase PCR (RT-PCR) was used to ensure that no full-length *AT4G11100* mRNA was present in the *at4g11100-e* plants. cDNA generated from *at4g11100-e* and Col-0 total RNA was subjected to PCR using *AT4G11100* primers specific to the 5' and 3' ends of the cDNA sequence (Figure 8). Amplification was only observed from the Col-0 cDNA, indicating that the T-DNA insert was sufficient to prevent the transcription of wild-type *AT4G11100* mRNA.

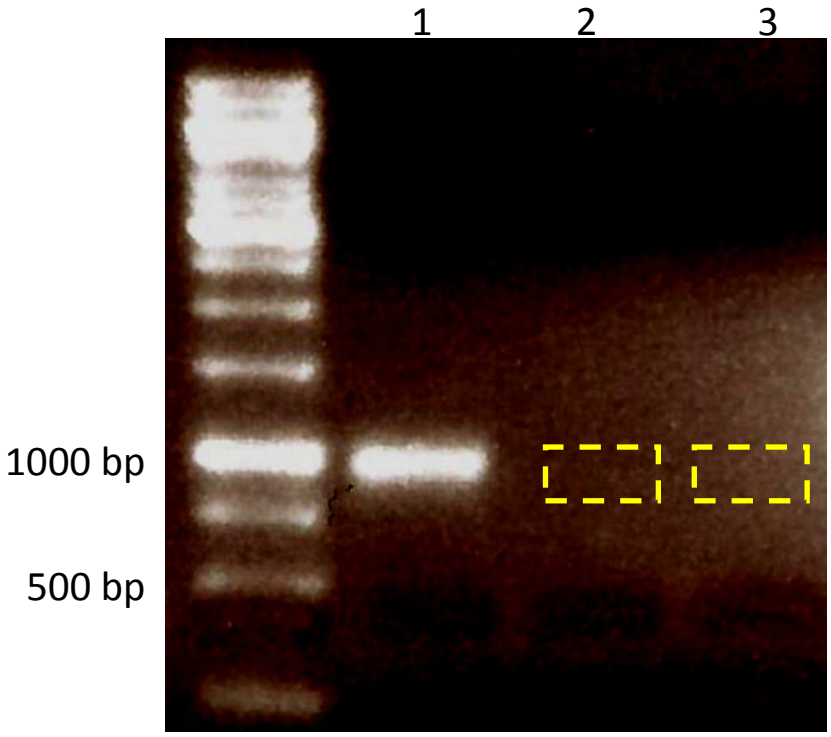

Figure 8| **Reverse transcriptase PCR (RT-PCR) of SALK_096586 plants homozygous for T-DNA insert.** PCR amplification of cDNA obtained from wild type Columbia (lane 1) and two plants from the homozygous T-DNA insertion line (lanes 2 and 3) using *AT4G11100* specific primers (At-LP & At-RP). The yellow boxes highlight the lack of amplification of cDNA from the two plants homozygous for the T-DNA insertion.

The identification of the *at4g11100-e* mutant was followed by a characterisation of its growth and resistance phenotypes. Considering the temperature dependent nature of *cir1* growth, the effects of temperature on the growth of the *at4g11100-p* and *at4g11100-e* mutants were investigated by growing both *at4g11100* mutants and Col-0 (*at4g11100-e* genetic background) at 18^{o}C, 22^{o}C, and 25^{o}C for 4 weeks. However, unlike *cir1*, neither *at4g11100* mutant displayed any reduction in growth at 18^{o}C or 22^{o}C when compared to Col-0 (data not shown). Next, 4 week old *at4g11100-p, at4g11100-e,* and Col-0 plants were infected with *Pst* DC3000, and bacterial growth was quantified 4 h and 48 h post infection (Figure 9). Both *at4g11100* mutants had significantly lower bacterial titres ($p < 0.05$) 48 h post infection than infected Col-0, with an approximate 10 fold reduction in bacterial titre; there was no significant difference in bacterial titre between the *at4g11100* mutants. Therefore it appears that although neither *at4g11100* mutant exhibits the temperature sensitive growth phenotype of *cir1*, both do show enhanced resistance to *Pst* DC3000 infection; and importantly, the *at4g11100-e* mutant displays the same phenotypes as *at4g11100-p,* indicating that this is likely due to disruption of *At4g11100*.

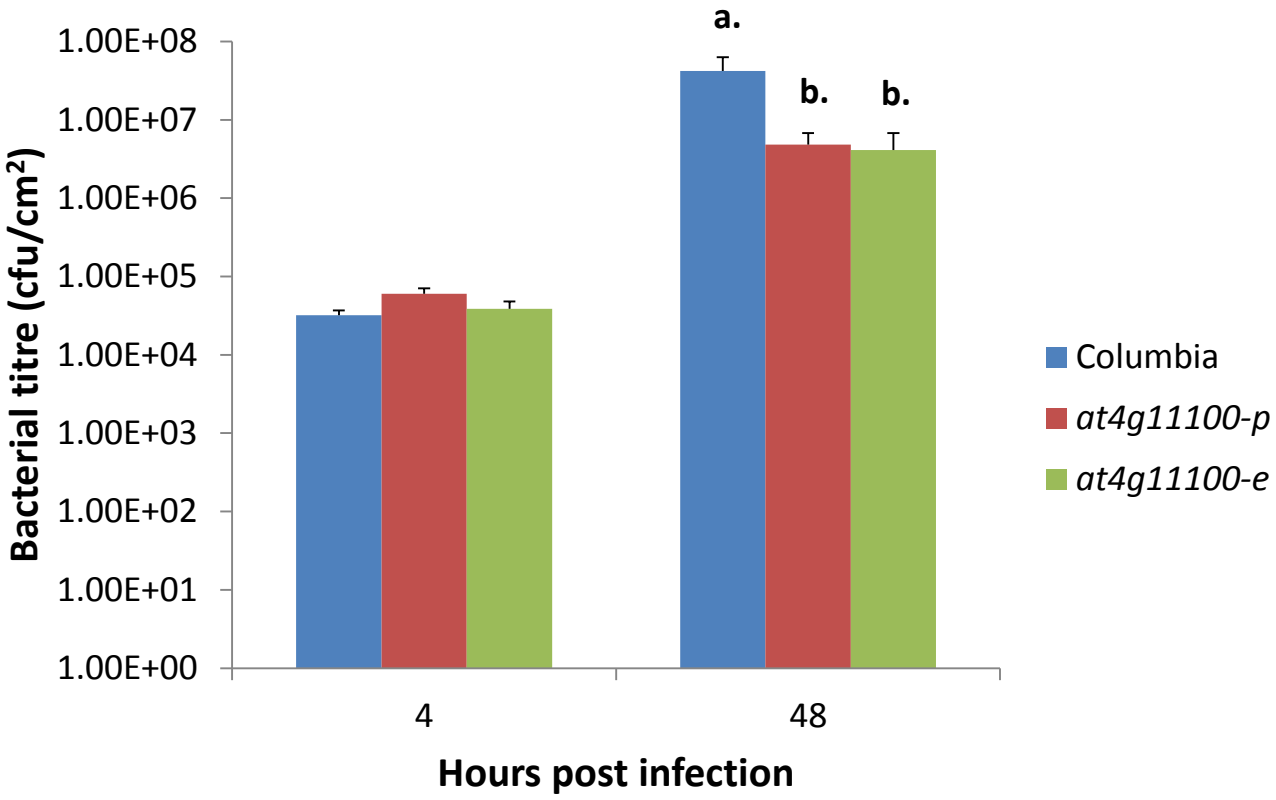

Figure 9| ***at4g11100*** **T-DNA insertion mutants display increased resistance to *P. syringae* infection.** Mean *P. syringae* titre (+SE, n = 5) in wild type Columbia (Col-0) and two AT4G11100 knockout lines 4 and 48 h post infection. Plants were grown for four weeks at 22°C prior to infection. Letters indicate significant differences ($p < 0.05$) determined by ANOVA with Fisher LSD. This experiment is representative of three independent experiments.

Heterologous expression of *AT4G11100* does not complement the *cir1* phenotype

If the *cir1* mutation is in *AT4G11100* then the introduction of a functional *AT4G11100* gene to the mutant should abolish the *cir1* phenotypes, including constitutive *PR-1* expression. To test this, the wild type *AT4G11100* open reading frame (ORF) was amplified from Col-0 *A. thaliana* cDNA and cloned into the pENTR™4 entry vector. The primers used to amplify and clone *AT4G11100* (Table 1) contained *EcoRI* and *BamHI* restriction enzyme sites, and so to confirm the presence of *AT4G11100* in pENTR™4, a double digest was performed (Figure

10A). Once the presence of *AT4G11100* in pENTR™4 had been confirmed, the *AT4G11100* coding region was sequenced to ensure that there were no mutations present in the gene, and the *AT4G11100* insert was transferred to the pFAST-G02 vector (Shimada, Shimada & Hara-Nishimura, 2010) through Gateway LR recombination. *E. coli* DH5α cells were then transformed with the resulting *pFAST-G02::AT4G11100* construct, and the presence of *AT4G11100* was again confirmed through a PCR (Figure 10B).

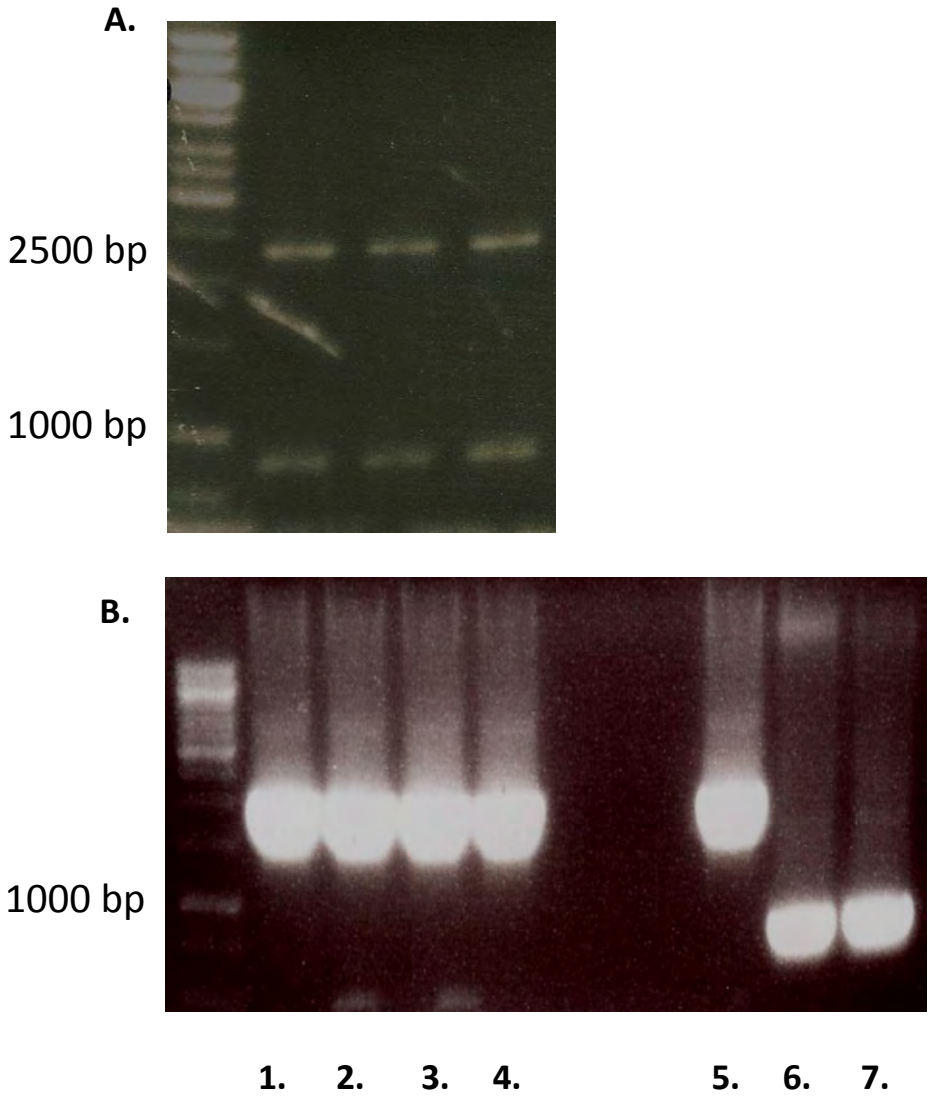

Figure 10| **Confirmation of *AT4G11100* in pENTR™4 and pFAST-G02.** A) Double digest of the *pENTR4::AT4G11100* vector with EcoRI and BamHI restriction enzymes. Bands correspond with the 864bp *AT4G11100* ORF and the 2400bp pENTR™4 vector backbone. B) Lanes 6 and 7 show PCR amplification of *AT4G11100* from the *pFAST-G02::AT4G11100* construct (using At-LP & At-RP primers). Bands correspond to the 864bp *AT4G11100* sequence. Lanes 1 – 5 show amplifications from non-related cloning experiments.

A GV3101 *Agrobacterium tumefaciens* strain was transformed with the *pFAST-G02::AT4G11100* construct, and the pFAST-G02 empty vector. These *A. tumefaciens* strains were in turn used to transform 6 week old *cir1* and *PR-1:LUC A. thaliana* plants. The presence of enhanced green fluorescent protein (eGFP) in the pFAST-G02 vector meant that transgenic seed from the transformed plants could be identified using a fluorescent microscope, where they fluoresced brightly after excitation at 395nm.

The *cir1* mutant was generated in a *PR-1:LUC* genetic background which contains a *PR-1* promoter transcriptionally fused to a luciferase reporter gene; this means that *PR-1* promoter activity can be inferred by the measurement of luciferase activity. The *cir1* mutant displays elevated levels of *PR-1* transcription, and therefore elevated luciferase activity when compared to its *PR-1:LUC* genetic background. With this in mind, the transgenic *cir1* and *PR-1:LUC* seeds were grown for two weeks at 22^{o}C before being assayed for luciferase activity, to determine if the presence of a functional *AT4G11100* gene would have any effect on *PR-1* promoter activity (Figure 11).

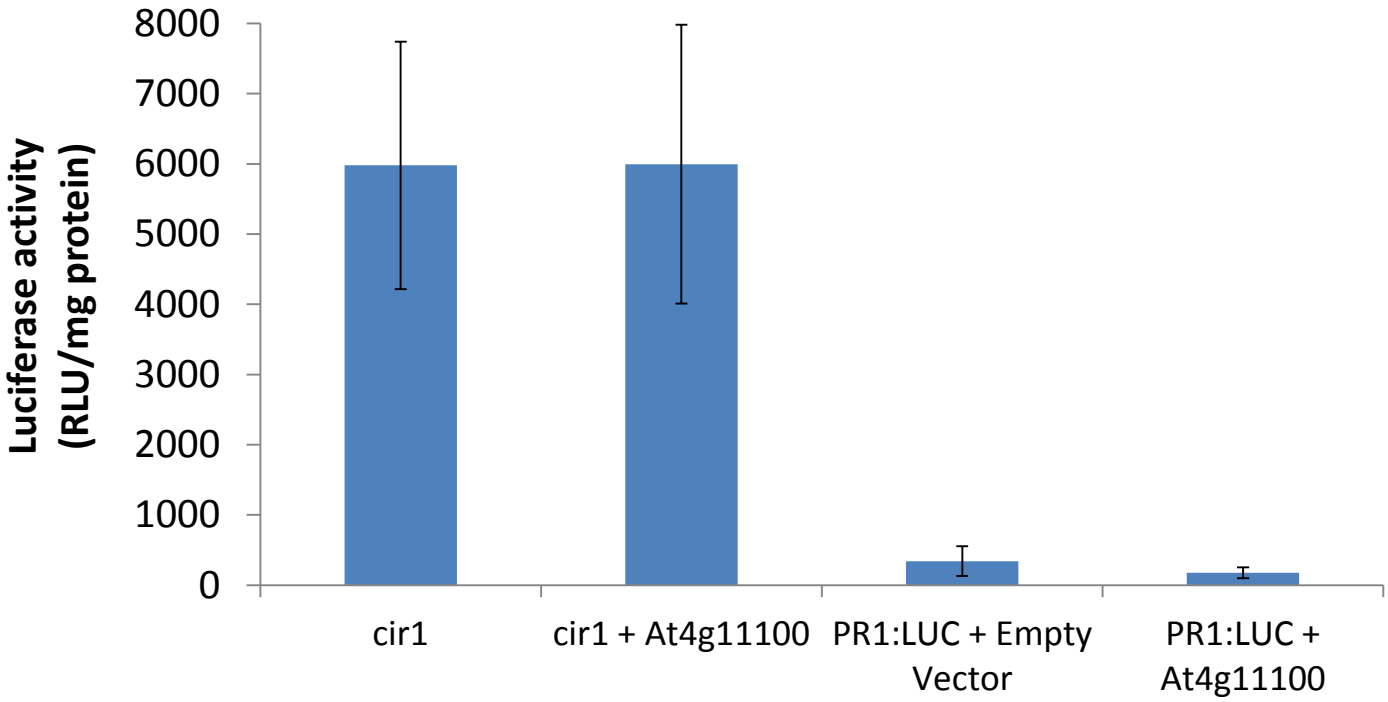

Figure 11| **Luciferase activity in *cir1* and *PR1:LUC* plants transformed with *AT4G11100*.** Mean luciferase activity from tissue of 2 week old plants was assayed in four plant lines: the *cir1* mutant (+SE, n = 3), *cir1* transformed with the *pFAST-G02::AT4G11100* construct (+SE, n = 2), *PR-1:LUC* transformed with the pFAST-G02 empty vector (+SE, n = 4), and *PR-1:LUC* transformed with the *pFAST-G02::AT4G11100* construct (+SE, n = 4). In vector-containing plant lines, biological replicates represent independent transformation events. Luciferase activity was normalised for total protein content using a Bradford assay. All plants were grown at 22°C.

Figure 11 clearly shows the elevated luciferase activity in *cir1* versus *PR-1:LUC* plants, as previously reported (Diener, 2012). However, the presence of *AT4G11100* has no effect on the luciferase activity of the *cir1* mutant, with no significant difference between luciferase activity in *cir1* and *cir1+AT4G11100* plants, suggesting that *AT4G11100* may not be the gene responsible for the *cir1* phenotype.

CIR1 and *AT4G11100* complementation - *AT4G11100* is not *CIR1*

A second experiment to determine whether the *AT4G11100* gene is in fact *CIR1* was performed; here, complementation was tested by cross pollinating the *at4g11100-e* and *cir1* mutants. Because the *cir1* mutation is recessive, two copies of the mutant allele are necessary to elicit the *cir1* phenotypes (i.e. constitutive expression of *PR-1*, and enhanced disease resistance); thus, in a genetic cross between *at4g11100-e* and *cir1*, if the mutation responsible for the *cir1* phenotype is present in the *AT4G11100* gene, then there will be constitutive expression of *PR-1* and high levels of luciferase activity. Conversely, if the mutation is in a different gene, no elevated expression of *PR-1* should occur and luciferase activity will be low (*i.e.* complementation has occurred).

Seeds from two *at4g11100-e* x *cir1* crosses were soil grown for two weeks at 22^{o}C before being assayed for luciferase activity. As before, the elevated *PR-1* transcription in *cir1* plants, and the low basal levels of *PR-1* transcription in *PR-1:LUC* plants, is reflected by the high and low levels of luciferase activity in *cir1* and *PR-1:LUC* respectively (Figure 12). Offspring from both *at4g11100-e* x *cir1* crosses displayed significantly lower luciferase activity when compared to those of *cir1* individuals; instead, offspring from both crosses were not significantly different from *PR-1:LUC* plants in luciferase activity, indicating that complementation had occurred. Thus, it seems likely that *CIR1* is not *AT4G11100.* Finally, DNA sequencing of the *AT4G11100* locus (including 1.5 kb of upstream sequence) in *cir1* showed no nucleotide differences compared to the wild type Col-0 sequence.

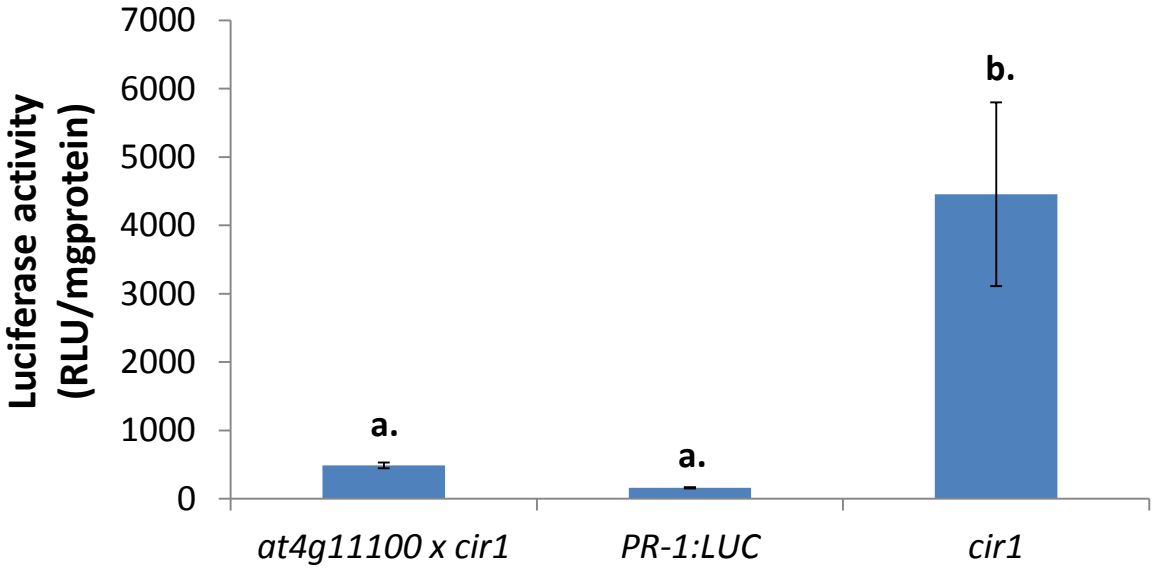

Figure 12**| Luciferase activity in the offspring of a cross between the *cir1* and *at4g11100-e* mutants.** Mean luciferase activity (+SE, n = 3) of tissue from 2 week old plants was assayed for luciferase activity in the *cir1* x *at4g11100* offspring, *PR-1:LUC* and *cir1*. Luciferase activity was normalised for total protein content using a Bradford assay. All plants were grown at 22°C. Letters indicate significant differences ($p < 0.05$) determined by ANOVA with Fisher LSD. This experiment is representative of two independent experiments.

Generation and characterisation of *AT4G11100* over expressers

Although *AT4G11100* is not *CIR1*, the *at4g11100* insertion mutants nonetheless exhibit increased resistance to *Pst* DC3000, suggesting that this gene may be involved in the negative regulation of innate immunity. Therefore, characterising the *AT4G11100* gene could yield valuable insight into the mechanisms underlying immunity in *A. thaliana*.

Because, like *CIR1*, *AT4G11100* is most likely a negative regulator of the immune response, the effect of over-expressing *AT4G11100* is an interesting avenue for investigation. The rationale behind creating *AT4G11100* over-expressing mutants was based on the hypothesis that over-expressing a negative regulator of plant immunity would inhibit a plant's ability to

resist disease. Therefore once such over-expresser plants were created, the effect of elevated *AT4G11100* expression on plant immunity and defence gene expression could be examined.

To generate transgenic plants over-expressing *AT4G11100,* the *pFAST-G02::AT4G11100* containing *A. tumefaciencs* strain described above was used to transform 4 week old Col-0 *A. thaliana* plants. The transgene inserted into the pFAST-G02 is under the control of a CaMV 35S viral promoter and is therefore expressed constitutively. The phosphinothricin-containing herbicide BASTA was sprayed on T_1 offspring of the transformed plants to select for transgenic individuals. T_2 seed was harvested from the T_1 survivors of herbicide selection, and again subjected to herbicide selection. T_2 lines that displayed a 3:1 survival ratio were allowed to set seed as this indicated that only a single insertion event had occurred. T_3 seedlings were treated with herbicide, and lines that displayed 100% survival were taken to be homozygous for the pFAST-G02::*AT4G11100* transgene. In this way 7 plant lines homozygous for the transgene were identified.

Transformation of plants using *A. tumefaciens* will result in random insertion of the transgene into the plant genome, and depending on where in the genome the transgene inserts, there will be different levels of expression of the insert. For this reason, it was important to isolate *pFAST-G02::AT4G11100* transgenic plant lines that originated from different transformation events and then to analyse their expression of *AT4G11100*. Expression of *AT4G11100* in seven homozygous T_3 transgenic plant lines arising from independent transformation events was assessed using qPCR (Figure 13). Relative to the *ACTIN2* reference gene, three *pFAST-G02::AT4G11100* transgenic plant lines (O-E 1, O-E 2,

and O-E 3) were identified as good candidates for further analysis based on their low, mid, and high *AT4G11100* expression levels respectively.

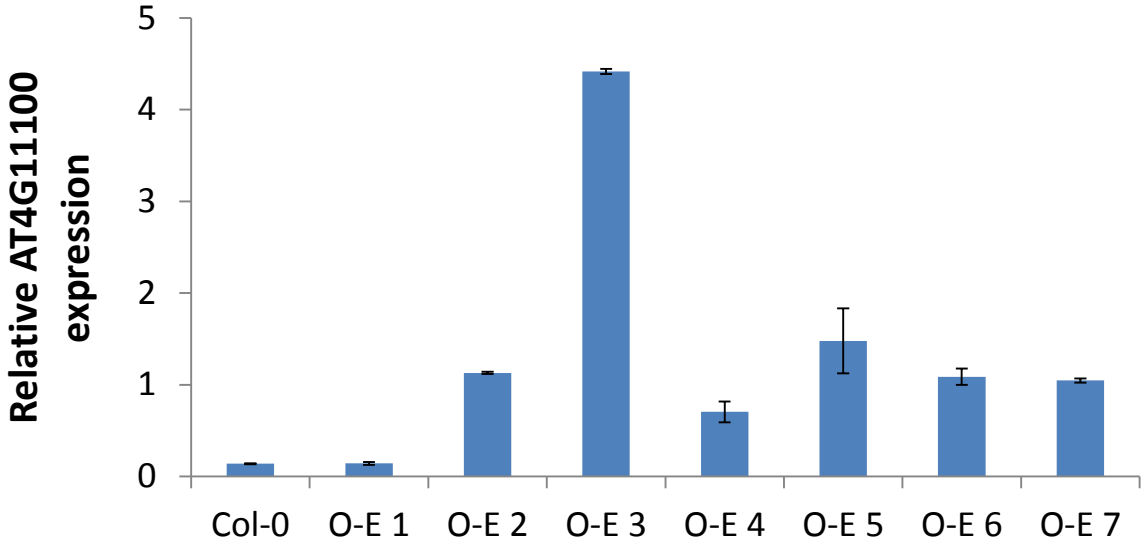

Figure 13| **Relative *AT4G11100* mRNA levels in *AT4G11100* over-expressing (O-E) plant lines .** O-E lines were made by transforming wild type Columbia (Col-0) plants with a *pFAST-G02::AT4G11100* construct; different O-E lines represent different transformation events. mRNA levels were normalised against *ACTIN*-2. Plants were grown for four weeks under a 16 hour light/8 hour dark cycle at 22°C.

O-E 1 had *AT4G11100* mRNA levels that were not significantly different to those in wild type Col-0 plants (and so was used as a vector control), but both O-E 2 and O-E 3 had considerably higher *AT4G11100* mRNA levels than Col-0, with 8 and 30 times more respectively. It was fortuitous to have found transgenic lines with this range of *AT4G11100* expression as it could make any AT4G11100 dose dependant effects easier to find.

AT4G11100* over-expressers display increased susceptibility to *Pseudomonas syringae

If *AT4G11100* is a negative regulator of plant immunity, then it is reasonable to expect that over-expression of *AT4G11100* will result in increased susceptibility to infection; the over-expression of a negative regulator might dampen the defence response mounted against pathogen attack. The effect of over-expression of *AT4G11100* on plant defence was examined by infecting 4 week old Col-0 and O-E plants with *Pst* DC3000 and quantifying bacterial growth 4 h and 48 h post infection (Figure 14).

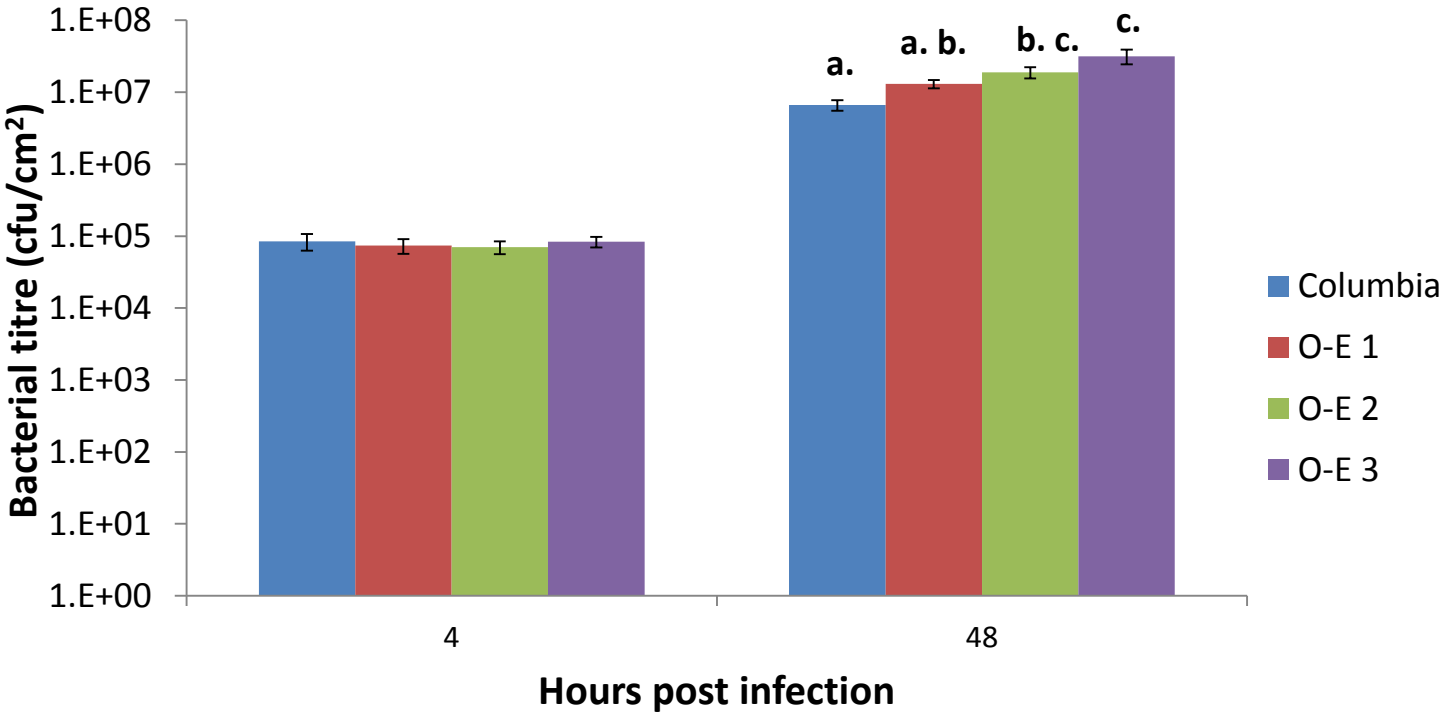

Figure 14| ***AT4G11100* over expressers (O-E) are more susceptible to *P. syringae* infection than wild type plants.** Mean *P. syringae* titre (+SE, n = 5) in wild type Columbia (Col-0) and three *AT4G11100* over expresser lines 4 and 48 h post infection. Plants were grown for four weeks at 22°C. Letters indicate significant differences ($p < 0.05$) determined by ANOVA with Fisher LSD. This experiment is representative of three independent experiments.

The *AT4G11100* over expressers displayed enhanced susceptibility to *Pst* DC3000 infection when compared to wild type Col-0, and interestingly, they did so in a manner mirroring the expression level of *AT4G11100*. At 48 h post infection, O-E 1, with *AT4G11100* expression no higher than Col-0, did not have a significantly higher bacterial titre than Col-0; whereas both O-E 2 and O-E 3, with significantly higher levels of *AT4G11100* expression, had significantly higher bacterial titres than Col-0 (three and five fold increases respectively). This would appear to confirm the role of *AT4G11100* as a negative regulator of the defence response, with increased expression of *AT4G11100* leading to suppression of immunity and therefore increased pathogen susceptibility.

Additional experiments were performed to determine if there is any association between expression of *AT4G11100* and defence gene expression, with the hypothesis that over-expression of At4g11000 would lead to reduced induction of defence genes after infection with *Pst* DC3000. Here, expression of the defence genes *PATHOGENISIS RELATED 2* (*PR2*) and *ISOCHORISMATE SYNTHASE 1* (*ICS1*) was examined in 4 week old O-E 1 and O-E 3 plant tissue infected with *Pst* DC3000, at 4h and 48h post infection. O-E 1 and O-E 3 were chosen for initial experiments as they display wild-type and highest expression of *AT4G11100* respectively, and behave differently in response to *Pst* DC3000 infection. Figures 15 shows preliminary data from the single experiment carried out.

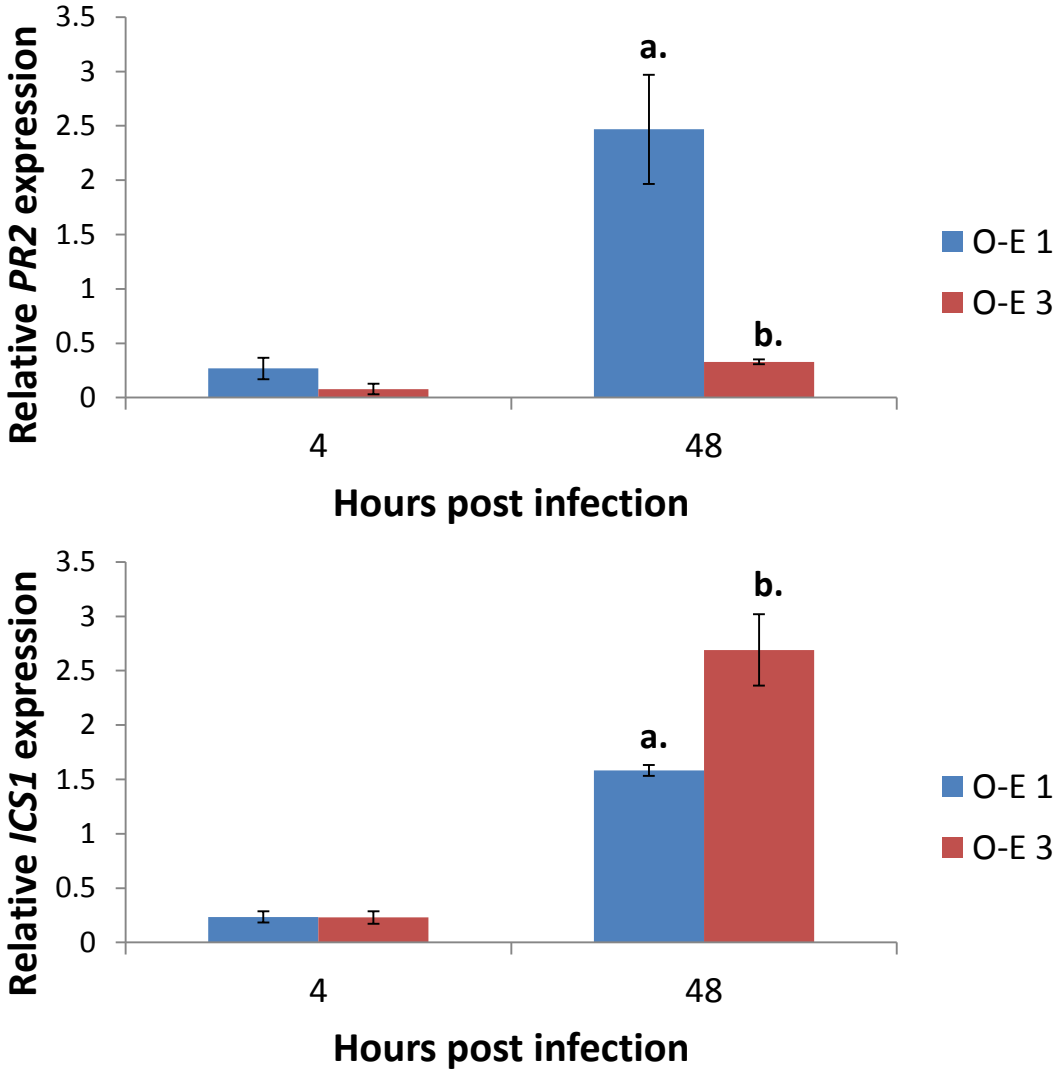

Figure 15| **Relative *PR2* and *ICS1* mRNA levels in two *AT4G11100* over-expressing (O-E) plant lines.** Relative expression of *PR2* (+SE, n = 3) and *ICS1* (+SE, n = 3) in two *AT4G11100* O-E lines, 4 and 48 h post infection with *P. syringae.* mRNA levels were normalised against *ACTIN*-2. Plants were grown for four weeks under a 16 hour light/8 hour dark cycle at 22°C. Letters indicate significant differences ($p < 0.05$) determined by ANOVA with Fisher LSD.

Initial data shows that *PR2* expression following infection with *Pst* DC3000 is significantly lower in O-E 3, where *AT4G11100* expression is higher, compared to O-E 1, where *AT4G11100* expression is at wild-type levels. This suggests that the elevated expression of *AT4G11100* in O-E 3 might be inhibiting the induction of *PR2* expression. The opposite trend is observed when *ICS1* expression is examined; *ICS1* is expressed at significantly lower levels after infection with *Pst* DC3000 when *AT4G11100* expression is low (O-E 1), compared to when *AT4G11100* expression is high (O-E 3).

Although these opposite patterns in defence gene expression might appear contradictory, the relative positions of *ICS1* and *PR2* in the defence signalling pathway might provide an explanation. *ICS1* is responsible for the synthesis of salicylic acid (SA), an important defence molecule that acts at the beginning of a signalling pathway that results in the expression of a large number of plant defence genes, including the *PR* defence genes (Yan & Dong, 2014). Additionally, in the absence of pathogen attack, *ICS1* expression is down regulated by the transcription factor CALMODULIN BINDING PROTEIN 60a (CBP60a) (Seyfferth & Tsuda, 2014). Figure 15 shows that over expression of *AT4G11100* lowers induction of *PR2*, but not that of *ICS1*. It is conceivable that AT4G11100 may prevent the negative regulation of *ICS1* by CBP60a and in this way block SA signalling downstream of SA production, but above PR2 production. This would explain the difference in expression observed between the two genes in *AT4G11100* over expressers, and potentially gives insight into where *AT4G11100* might act in its regulation of plant immunity. However, these results are preliminary and the experiments need to be repeated, specifically with the inclusion of expression data from wild type plants.

***AT4G11100* over-expresser has distinct leaf morphology**

While the *AT4G11100* over expressing O-E 3 plant line displayed increased susceptibility to *P. syringae* infection, it is also worth noting that O-E 3 plants exhibited a leaf morphology distinct from both the other over expressing lines (O-E 1 & O-E 2; both of which express *AT4G11100* at considerably lower levels than O-E 3), and wild type plants. At 4 weeks, compared to both wild type Col-0 and other over expresser lines, O-E 3 plant leaves have more serrated edges, particularly in younger leaves (Figure 16). The shapes of the O-E 3 leaves are noticeably different from wild type, and also appear to have a rougher surface.

Figure 16| **Distinct leaf morphology of plants highly over expressing *AT4G11100* (O-E 3).** Leaves are arrayed from oldest to youngest (left to right). Arrays from wild type Columbia (Col-0) and a moderate *AT4G11100* over expresser (O-E 2) are shown. Plants were grown for four weeks under a 16 hour light/8 hour dark cycle at 22°C.

The surface of O-E 3 plant leaves was examined using a dissecting microscope, and it became apparent that the rough texture of O-E 3 leaves visible in the leaf arrays is due to an increased number of trichomes (Figure 17A). The number of trichomes per leaf area was determined, and it was clear that O-E 3 had a significantly higher number of trichomes per leaf area (approximately double) than both wild type and other *AT4G11100* over expressing plants (Figure 17B).

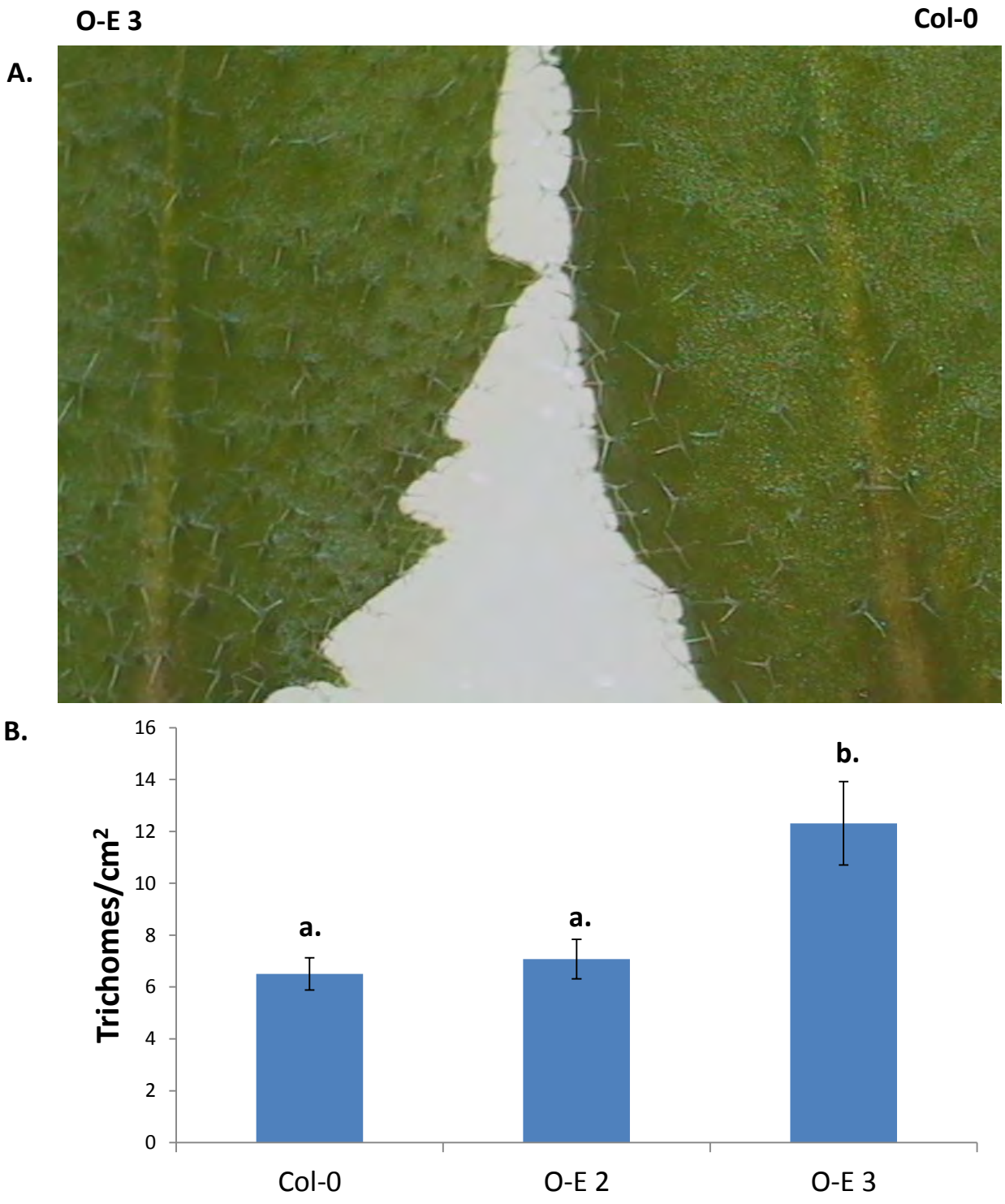

Figure 17| **The highest *AT4G11100* over expresser (O-E 3) has more trichomes than wild type plants.** Leaf 10 from O-E 3 and Columbia (Col-0) was examined under a dissecting microscope (A) and the number of trichomes per cm^2 (+SE, n = 5) was calculated for leaf 6 from Col-0, O-E 2 and O-E 3 (B). Letters indicate significant differences ($p < 0.05$) determined by ANOVA with Fisher LSD. Plants were grown for four weeks under a 16 hour light/8 hour dark cycle at 22°C.

It is important to note that while the distinct morphological phenotype of O-E 3 is interesting, the role of *AT4G11100* in generating the phenotype should not be over stated. The data show that O-E 3 has an increased number of trichomes compared to wild type, not necessarily that increased expression of *AT4G11100* leads to higher numbers of trichomes. The high number of trichomes present in O-E 3 leaves might be due to the position in the genome that the *pFAST-G02::AT4G11100* construct inserted. If the construct happened to disrupt a locus involved in leaf development, this might explain the trichome phenotype. However, if the increased expression of *AT4G11100* does lead to higher numbers of trichomes, this could provide additional insight into the function and role of *AT4G11100*. To more definitively determine the effect of *AT4G11100* expression on leaf morphology it would be useful to analyse additional independent *AT4G11100* over expressers with high transgene expression from a separate transformation event.

However, it is interesting to note that in a series of yeast two hybrid assays AT4G11100 was found to interact with two NB-LRR RLKs, AT2G36570 and AT3G50230 (Mukhtar *et al*., 2011), both of which are implicated in plant development. And it has been suggested that AT2G36570 (*PXC PXY/TDR-CORRELATED GENE 1*, or *PXC1*) in particular is involved in plant vascular development and secondary cell wall formation in xylem fibres (Wang *et al*., 2013). It is possible that altered levels of AT4G11100 may disrupt function of these NB-LRR RLKs, the first step towards testing this would be to determine whether AT4G11100 actually interacts with AT2G36570 and AT3G50230 *in planta*. One means of testing such an interaction would be through the use of a bimolecular fluorescence complementation assay in which two halves of a fluorescent protein (yellow fluorescent protein, or YFP, as

AT4G11100:GFP may be unstable – see below) are fused to AT4G11100 and an RLK, and if they interact *in planta*, the two halves of YFP will come together and fluoresce.

Subcellular localization of AT4G11100

It seems likely that *AT4G11100* plays a role in regulating plant immunity; manipulating the expression of *AT4G11100* has a clear impact of the ability of *A. thaliana* to resist bacterial infection. Understanding the mechanisms governing how AT4G11100 behaves on a subcellular level is therefore of great interest, particularly with regard to how AT4G11100 may regulate the immune response. With this in mind, finding where AT4G11100 localises in the cell could help to elucidate how AT4G11100 functions.

To determine where AT4G11100 localises, a *pk7FGW2::AT4G11100* vector was created through Gateway LR recombination of the *AT4G11100* containing pENTR™4 vector (see page 8 above) with the pk7FGW2 destination vector. The resulting *pk7FGW2::AT4G11100* vector allows for the translational fusing of the C- terminus of *AT4G11100* with *eGFP*, resulting in an AT4G11100::eGFP fusion protein when expressed. The *pk7FGW2::AT4G11100* vector was sequenced to confirm that the GFP tag was in frame with *AT4G11100* and transfected into two week old maize protoplasts which were then examined under a confocal microscope (Figure 18).

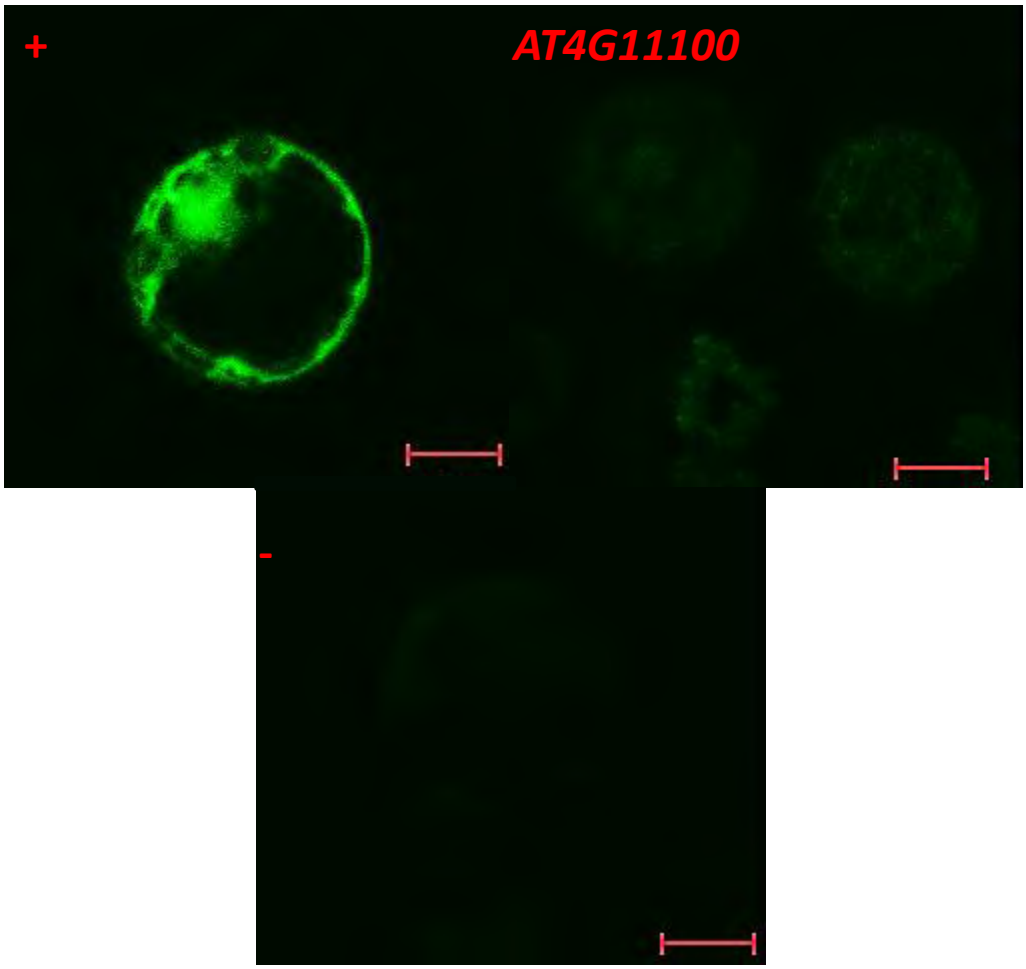

Figure 18| **No fluorescence in *pk7FGW2::AT4G11100* transfection of maize protoplasts.** Two week old maize protoplasts transfected with either *pk7FGW2::IMPL2*$_{-1-60}$ as a positive control (+), the *pk7FGW2::AT4G11100* fusion vector (*AT4G11100*), or transfection solution without DNA as a negative control(-). The *IMPL2*$_{-1-60}$ gene has been truncated so that its protein will not contain plastid transit peptides and thus localises in the cytoplasm. Green fluorescence was detected using a confocal microscope after laser excitation at 395nm. Plants were grown under a 16 hour light/8 hour dark cycle at 22°C. Red bars indicate a distance of 10µm.

The transfection was successful with the *pk7FGW2::MYOINOSITOL MONOPHOSPHATASE-LIKE2* (*IMPL2*)$_{-1-60}$ construct acting as a positive control. The *IMPL2*$_{-1-60}$ gene has been truncated to remove the first 60 amino acids coded; this region contains the transit peptides necessary for IMPL2 plastid localisation, and thus the truncated IMPL2$_{-1-60}$:eGFP fusion protein will localise in the cytoplasm (Petersen *et al*., 2010). The *pk7FGW2::IMPL2*$_{-1-60}$ transfection showed clear green fluorescence in the protoplast cytoplasm. Unfortunately,

none of the protoplasts transfected with the *pk7FGW2::AT4G11100* fusion vector showed any green fluorescence above background levels. The transfection experiments were repeated a number of times, using both *A. thaliana* and maize protoplasts; however green fluorescence was never observed in protoplasts transfected with *pk7FGW2::AT4G11100*.

Concurrently with the transfection experiments, the creation of stable plant lines containing the *pk7FGW2::AT4G11100* fusion vector was carried out. The rationale behind the creation of these transgenic plants was that *in vivo* observations of AT4G11100::eGFP might be possible. Once the transfections failed to produce any information on the subcellular localisation of AT4G11100, it was hoped that the *pk7FGW2::AT4G11100* containing plants might yield better results.

Therefore, a GV3101 *A. tumefaciens* strain was transformed with *pk7FGW2::AT4G11100*, which was in turn used to transform 4 week old wild type *A. thaliana* plants. The pk7FGW2 vector contains a kanamycin resistance gene that could be used to select for positive transformants, and so multiple homozygous *pk7FGW2::AT4G11100* containing lines, from various separate transformation events, were then isolated through several generations of kanamycin selection.

Once plants homozygous for the *pk7FGW2::AT4G11100* vector had been identified, whole leaves from various lines at various stages of development were examined under a confocal microscope. Figure 19 shows images taken of a two week old transgenic plant; no GFP fluorescence above background levels was detected at any of the developmental stages examined. The same result was found in all lines studied.

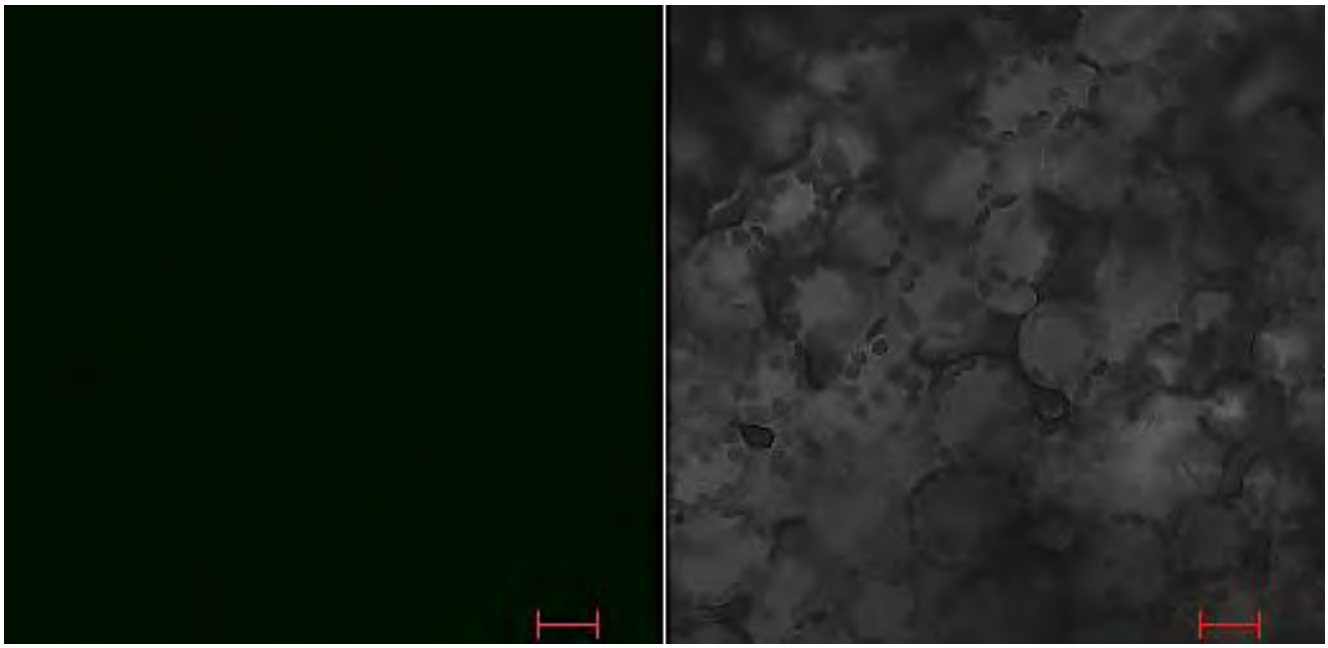

Figure 19| **No fluorescence in transgenic *pk7FGW2::AT4G11100* containing plant leaves.** Leaves of two week old transgenic *A. thaliana* plants containing the *pk7FGW2::AT4G11100* fusion vector, viewed with a confocal microscope. The left hand panel shows the leaf under laser excitation at 395nm. The right hand panel is the same section with no light excitation. Plants were grown under a 16 hour light/8 hour dark cycle at 22°C. Red bars indicate a distance of 20µm.

The lack of fluorescence in a single *pk7FGW2::AT4G11100* transgenic plant line might be due to the insertion of the vector in a transcriptionally silent region of the genome; however, because multiple transgenic plant lines had been created from multiple insertion events, it seemed unlikely that the *pk7FGW2::AT4G11100* construct was being silenced in all lines. A western blot was performed using total protein extracted from *pk7FGW2::AT4G11100* transgenic plant lines and eGFP antibodies in an effort to determine whether the eGFP fusion protein was actually expressed in the transgenic plant lines (Figure 20). However, none of the several independently transformed lines tested exhibited any binding of eGFP antibody, suggesting that no eGFP was being produced in any of the transgenic plant lines.

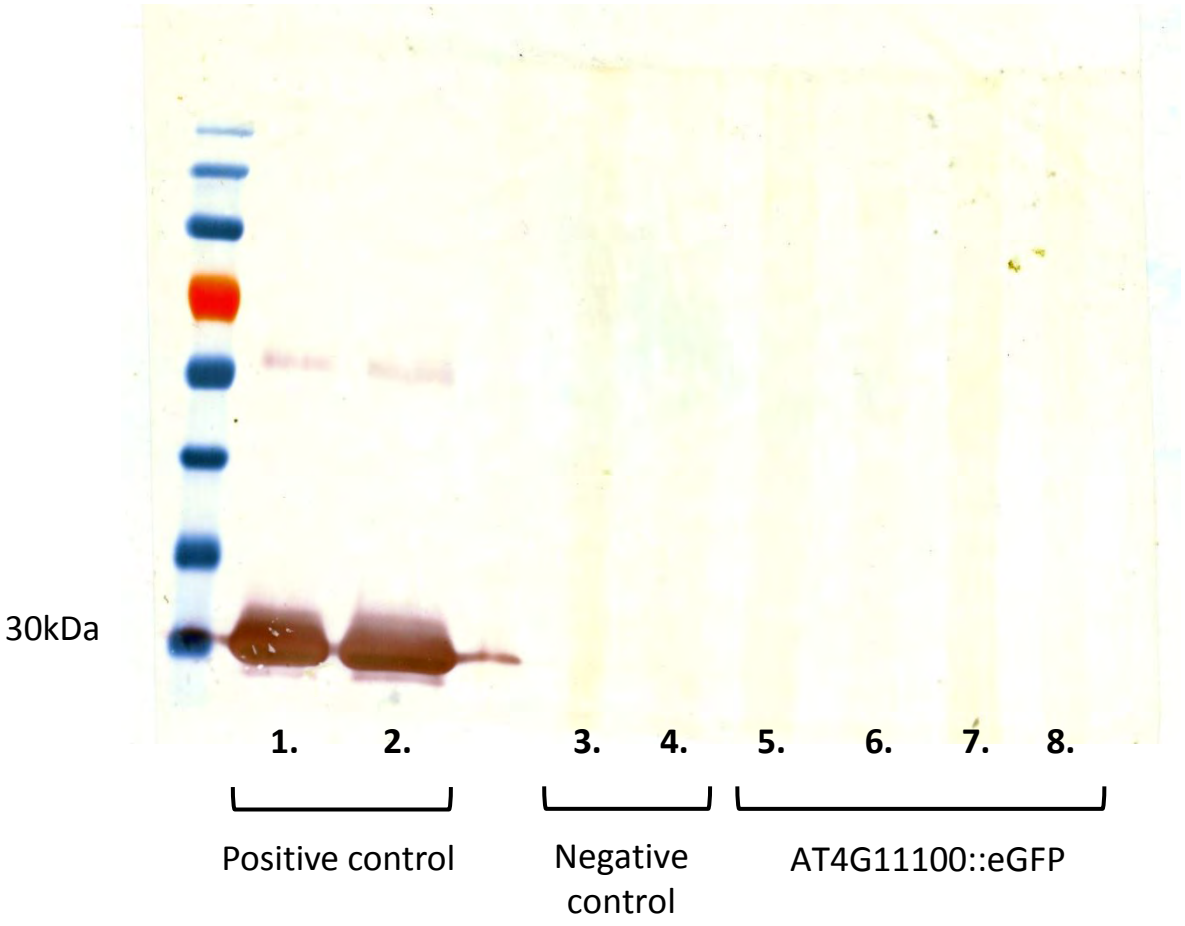

Figure 20| **eGFP protein was not detected in *pk7FGW2::AT4G11100* containing transgenic plant lines.** 40mg total protein was extracted from 4 week old *A. thaliana* plants containing the *pk7FGW2::AT4G11100* fusion vector (4 independent lines), and probed with an eGFP antibody in a Western blot (lanes 5 – 8). Bacterially expressed eGFP was used as a positive control (lanes 1 and 2), and total protein from 4 week old Columbia plants used as a negative control (lanes 3 and 4). A 30kDa band corresponds with the size of the eGFP protein.

The absence of eGFP in any of the *pk7FGW2::AT4G11100* transgenic plant lines explains why no fluorescence was detected in these plants; however, the cause of the absence of eGFP in these plants is not clear. A total lack of expression of the *pk7FGW2::AT4G11100* construct in the transgenic plants seems an unlikely cause as all the stable lines exhibit kanamycin resistance, which is conferred by the vector. If the expression of the *AT4G11100::eGFP* fusion is being somehow prevented, this would offer a reason for the failure of eGFP fluorescence. Equally, if the AT4G11100::eGFP protein fusion is unstable, this would explain

why both the protoplast transfections and the transgenic plant lines do not fluoresce. In either case, further experiments would need to be performed to determine why the eGFP is not being produced. RT-PCR analysis of the transgenic plant lines would reveal if the *AT4G11100::eGFP* is actually being transcribed. Another course of action may be to create another fusion of AT4G11100 and eGFP, but as an N-terminal fusion as opposed to the C-terminal fusion performed here; this might circumvent any stability issue that may be associated with the current fusion protein.

Chapter 4: Conclusion

Plants possess a complex system of defence to prevent pathogen establishment, including two branches of innate immunity. Tight control of these defence systems is necessary to ensure appropriate timing and severity of immune responses in reaction to specific pathogens, including suppression of the immune system in the absence of pathogen attack. The *A. thaliana cir1* null mutant is characterised by constitutive expression of defence genes, and enhanced resistance to *Pst* DC3000, suggesting that *CIR1* is a likely negative regulator of defence (Murray *et al*., 2002).

Relatively early in the course of this project it was discovered the *cir1* mutant displays a temperature sensitive growth phenotype (Figure 3). This led to an investigation into the effects of temperature on the *cir1* defence phenotype, which revealed that the *cir1* defence phenotype is actually temperature dependent (Figure 4). Efforts to identify the gene responsible for *CIR1* have previously led to the identification of *AT4G11100* as a likely *CIR1* candidate (Carstens, 2008; Diener, 2012), and this continued to appear likely as *at4g11100* T-DNA knockouts displayed a similar defence phenotype to *cir1* (Figure 9). However, through complementation tests and genetic crosses (Figure 11 & Figure 12), this project has revealed that *AT4G11100* is not *CIR1*.

The creation and analysis of *AT4G11100* over-expressers shows that increased expression of *AT4G11100* causes increased susceptibility to infection by *Pst* DC3000 (Figure 14), suggesting that, like *cir1*, *AT4G11100* is a likely negative regulator of defence. Additionally, a transgenic plant line with high levels of *AT4G11100* expression displays distinct leaf

morphology, with serrated edges (Figure 16) and increased trichome density (Figure 17). This may implicate *AT4G11100* in plant development, though independent *AT4G11100* over-expressing lines would need to be created and analysed to confirm this.

Unfortunately, subcellular localisation of the AT4G11100 protein could not be determined despite efforts to create an AT4G11100:eGFP fusion protein (Figure 18 & Figure 19), potentially as a result of problematic expression or stability of the fusion.

The creation and analysis of independent *AT4G11100* over-expressing plant lines could help determine if the distinct leaf morphology seen in the over-expresser line described in this project is actually due to high *AT4G11100* mRNA/protein levels. Additionally, further examination of the two NB-LRR RLKs (AT2G36570 and AT3G50230) that are thought to interact with AT4G11100 (Mukhtar *et al*., 2011) could prove useful, specifically in determining if they do in fact interact with AT4G11100 *in planta* via a bimolecular fluorescence complementation assay, as the yeast two hybrid method used by Mukhtar *et al.* (2011) often gives false positives. The qPCR experiments examining relative expression of *ICS1* and *PR2* in an *AT4G11100* over-expresser (Figure 15) need to be repeated to confirm that the expression data found is significant. Furthermore, it may be interesting to investigate whether AT4G11100 interacts with the negative regulator of *ICS1,* CBP60a, and possibly explain why *ICS1* and *PR2* expression differs in *AT4G11100* over-expressing plant lines. To help dissect where in the SA defence pathway *AT4G11100* is exerting a negative effect, expression levels of more defence genes in *AT4G11100* over-expressers could be examined.

Overall, this study has identified novel, temperature dependant phenotypes of the *cir1* mutant; ruled out *AT4G11100* as the gene responsible for the *cir1* phenotypes; and implicated *AT4G11100* in the negative regulation of the plant immune system. Although further studies will need to be carried out to identify *CIR1*, the findings presented here contribute to the understanding of the complex defence systems utilised by *A. thaliana* in defence against pathogen attack.

Chapter 5: References

Abramovitch, R.B. & Martin, G.B. 2004. Strategies used by bacterial pathogens to suppress plant defenses. *Current Opinion in Plant Biology*. 7:356–364.

Asai, T., Tena, G., Plotnikova, J., Willmann, M.R., Chiu, W.L., Gomez-Gomez, L., Boller, T., Ausubel, F.M., *et al*. 2002. MAP kinase signalling cascade in Arabidopsis innate immunity. *Nature*. 415:977–983.

Boller, T. & Felix, G. 2009. A renaissance of elicitors: perception of microbe-associated molecular patterns and danger signals by pattern-recognition receptors. *Annual Review of Plant Biology*. 60:379–406.

Carstens, M. 2008. Understanding the mechanisms of *cir1* disease resistance in *Arabidopsis thaliana*. PhD thesis. University of Cape Town.

Chinchilla, D., Zipfel, C., Robatzek, S., Kemmerling, B., Nürnberger, T., Jones, J.D.G., Felix, G. & Boller, T. 2007. A flagellin-induced complex of the receptor FLS2 and BAK1 initiates plant defence. *Nature*. 448:497–500.

Chomczynski, P. and Mackey, K. 1995. Short technical reports. Modification of the TRI reagent procedure for isolation of RNA from polysaccharide- and proteoglycan-rich sources. *Biotechniques*. 19:942-945.

Clough, S.J., Bent, A.F., 1998. Floral dip: a simplified method for *Agrobacterium*-mediated transformation of *Arabidopsis thaliana. The Plant Journal.* 16(6), p.735–43.

Cohen, J.E. 2003. Human population: the next half century. *Science*. 302:1172–1175.

Colcombet, J. & Hirt, H. 2008. Arabidopsis MAPKs: a complex signalling network involved in multiple biological processes. *The Biochemical Journal*. 413:217–226.

Dangl, J.L. & Jones, J.D. 2001. Plant pathogens and integrated defence responses to infection. *Nature*. 411:826–833.

Dellaporta, S.L., Wood, J., Hicks, J.B., 1983. A plant DNA minipreparation: Version 2. *Plant Molecular Biology Reporter* 1, 4, p.19–22.

Diener, A. 2012. Identification of the cir1 disease resistance gene in Arabidopsis. MSc dissertaion. University of Cape Town.

Dodds, P.N. & Rathjen, J.P. 2010. Plant immunity: towards an integrated view of plant-pathogen interactions. *Nature Reviews. Genetics*. 11(August):539–548.

Dodds, P.N., Lawrence, G.J., Catanzariti, A.-M., Teh, T., Wang, C.-I. a, Ayliffe, M. a, Kobe, B. & Ellis, J.G. 2006. Direct protein interaction underlies gene-for-gene specificity and coevolution of the flax resistance genes and flax rust avirulence genes. *Proceedings of the National Academy of Sciences of the United States of America*. 103:8888–8893.

Dong, X. 2004. NPR1, all things considered. *Current Opinion in Plant Biology*. 7:547–552.

Durrant, W.E. & Dong, X. 2004. Systemic acquired resistance. *Annual Review of Phytopathology*. 42:185–209.

Eitas, T.K. & Dangl, J.L. 2010. NB-LRR proteins: Pairs, pieces, perception, partners, and pathways. *Current Opinion in Plant Biology*. 13:472–477.

Felix, G. & Boller, T. 2003. Molecular sensing of bacteria in plants: The highly conserved RNA-binding motif RNP-1 of bacterial cold shock proteins is recognized as an elicitor signal in tobacco. *Journal of Biological Chemistry*. 278:6201–6208.

Fu, Z.Q. & Dong, X. 2013. Systemic acquired resistance: turning local infection into global defense. *Annual Review of Plant Biology*. 64:839–63.

Fu, Z.Q., Yan, S., Saleh, A., Wang, W., Ruble, J., Oka, N., Mohan, R., Spoel, S.H., *et al*. 2012. NPR3 and NPR4 are receptors for the immune signal salicylic acid in plants. *Nature*. 486(7402):228–232.

Garrett, K.A., Dendy, S.P., Frank, E.E., Rouse, M.N. & Travers, S.E. 2006. Climate change effects on plant disease: genomes to ecosystems. *Annual Review of Phytopathology*. 44:489–509.

Godfray, H.C.J., Beddington, J.R., Crute, I.R., Haddad, L., Lawrence, D., Muir, J.F., Pretty, J., Robinson, S., *et al*. 2010. Food security: the challenge of feeding 9 billion people. *Science*. 327:812–818.

Gómez-Gómez, L. 2004. Plant perception systems for pathogen recognition and defence. *Molecular Immunology*. 41:1055–1062.

Gómez-Gómez, L. & Boller, T. 2000. FLS2: An LRR Receptor–like Kinase Involved in the Perception of the Bacterial Elicitor Flagellin in Arabidopsis. *Molecular Cell*. 5:1003–1011.

Gómez-Gómez, L., Bauer, Z. & Boller, T. 2001. Both the extracellular leucine-rich repeat domain and the kinase activity of FSL2 are required for flagellin binding and signaling in Arabidopsis. *The Plant Cell*. 13:1155–1163.

Gou, M., Su, N., Zheng, J., Huai, J., Wu, G., Zhao, J., He, J., Tang, D., *et al*. 2009. An F-box gene, CPR30, functions as a negative regulator of the defense response in Arabidopsis. *Plant Journal*. 60:757–770.

He, P., Shan, L., Lin, N.C., Martin, G.B., Kemmerling, B., Nürnberger, T. & Sheen, J. 2006. Specific Bacterial Suppressors of MAMP Signaling Upstream of MAPKKK in Arabidopsis Innate Immunity. *Cell*. 125:563–575.

Van der Hoorn, R. a L. & Kamoun, S. 2008. From Guard to Decoy: a new model for perception of plant pathogen effectors. *The Plant Cell*. 20:2009–2017.

Holsters, M., Silva, B., Van Vliet, F., Genetello, C., De Block, M., *et al*, 1980. The functional organization of the nopaline *A. tumefaciens* plasmid pTiC58. *Plasmid*, 3(2), p.212–30.

Horbach, R., Navarro-Quesada, A.R., Knogge, W. & Deising, H.B. 2011. When and how to kill a plant cell: Infection strategies of plant pathogenic fungi. *Journal of Plant Physiology*. 168:51–62.

Jones, D.A. & Takemoto, D. 2004. Plant innate immunity - Direct and indirect recognition of general and specific pathogen-associated molecules. *Current Opinion in Immunology*. 16:48–62.

Jones, J.D.G. & Dangl, J.L. 2006. The plant immune system. *Nature*. 444:323–329.

Katagiri, F., Thilmony, R., He, S.Y., 2002. The *Arabidopsis Thaliana-Pseudomonas Syringae* interaction. *The Arabidopsis Book*, 20(1), p.1-39.

Kim, S.H., Gao, F., Bhattacharjee, S., Adiasor, J. a., Nam, J.C. & Gassmann, W. 2010. The arabidopsis resistance-like gene SNC1 is activated by mutations in SRFR1 and contributes to resistance to the bacterial effector AvrRps4. *PLoS Pathogens*. 6.

King, E.O., Ward, M.K., Raney, D.E., 1954. Two simple media for the demonstration of phycocyanin and fluorescin. *Journal of Laboratory and Clinical Medicine*, 44, p.301–307.

Lin, N.-C. & Martin, G.B. 2007. Pto- and Prf-mediated recognition of AvrPto and AvrPtoB restricts the ability of diverse pseudomonas syringae pathovars to infect tomato. *Molecular Plant-Microbe Interactions.* 20:806–815.

Liu, J., Elmore, J.M., Lin, Z.J.D. & Coaker, G. 2011. A receptor-like cytoplasmic kinase phosphorylates the host target RIN4, leading to the activation of a plant innate immune receptor. *Cell Host and Microbe*. 9:137–146.

Mackey, D., Belkhadir, Y., Alonso, J.M., Ecker, J.R. & Dangl, J.L. 2003. Arabidopsis RIN4 is a target of the type III virulence effector AvrRpt2 and modulates RPS2-mediated resistance. *Cell*. 112:379–389.

Meng, X. & Zhang, S. 2013. MAPK cascades in plant disease resistance signaling. *Annual Review of Phytopathology*. 51:245–66.

Mukhtar, M.S., Carvunis, A.-R., Dreze, M., Epple, P., Steinbrenner, J., Moore, J., Tasan, M., Galli, M., *et al*. 2011. Independently evolved virulence effectors converge onto hubs in a plant immune system network. *Science.* 333:596–601.

Murray, S.L., Thomson, C., Chini, A., Read, N.D. & Loake, G.J. 2002. Characterization of a novel, defense-related Arabidopsis mutant, cir1, isolated by luciferase imaging. *Molecular Plant-Microbe Interactions.* 15:557–566.

Mysore, K.S. & Ryu, C.-M. 2004. Nonhost resistance: How much do we know? *Trends in Plant Science*. 9(2):97–104.

Nakagami, H., Pitzschke, A. & Hirt, H. 2005. Emerging MAP kinase pathways in plant stress signalling. *Trends in Plant Science*. 10:339–346.

Nuernberger, T. & Lipka, V. 2005. Non-host resistance in plants: new insights into an old phenomenon. *Molecular Plant Pathology*. 6:335–345.

Oh, C.-S. & Martin, G.B. 2011. Effector-triggered immunity mediated by the Pto kinase. *Trends in Plant Science*. 16:132–140.

Petersen, L.N., Marineo, S., Mandalà, S., Davids, F., Sewell, B.T. & Ingle, R.A. 2010. The missing link in plant histidine biosynthesis: *Arabidopsis* myoinositol monophosphatase-like2 encodes a functional histidinol-phosphate phosphatase. *Plant Physiology*. 152:1186–1196.

Sambrook, J., Fritsch, E.F., Maniatis, T., 1989. *Molecular cloning: a laboratory manual* 2nd Edition, Cold Spring Harbour, New York: Cold Spring Harbor Laboratory Press.

Scholl, R.L., May, S.T. & Ware, D.H. 2000. Seed and molecular resources for Arabidopsis. *Plant Physiology*. 124:1477–1480.

Serghini, M.A., Ritzenthaler, C. & Pinck, L. 1989. A rapid and efficient 'miniprep' for isolation of plasmid DNA. *Nucl. Acids Res.* 17:3604

Seyfferth, C. & Tsuda, K. 2014. Salicylic acid signal transduction: the initiation of biosynthesis, perception and transcriptional reprogramming. *Frontiers in Plant Science*. 5:1–10.

Shimada, T.L., Shimada, T. & Hara-Nishimura, I. 2010. A rapid and non-destructive screenable marker, FAST, for identifying transformed seeds of Arabidopsis thaliana. *Plant Journal*. 61:519–528.

Strange, R.N. & Scott, P.R. 2005. Plant disease: a threat to global food security. *Annual Review of Phytopathology*. 43:83–116.

Trujillo, M., Ichimura, K., Casais, C. & Shirasu, K. 2008. Negative Regulation of PAMP-Triggered Immunity by an E3 Ubiquitin Ligase Triplet in Arabidopsis. *Current Biology*. 18:1396–1401.

Wang, J., Kucukoglu, M., Zhang, L., Chen, P., Decker, D., Nilsson, O., Jones, B., Sandberg, G., *et al*. 2013. The Arabidopsis LRR-RLK, PXC1, is a regulator of secondary wall formation correlated with the TDIF-PXY/TDR-WOX4 signaling pathway. *BMC Plant Biology*. 13:94.

Wang, Y., Bao, Z., Zhu, Y. & Hua, J. 2009. Analysis of temperature modulation of plant defense against biotrophic microbes. *Molecular Plant-Microbe Interactions*. 22:498–506.

Whalen, M.C., Innes, R.W., Bent, a F. & Staskawicz, B.J. 1991. Identification of Pseudomonas syringae pathogens of Arabidopsis and a bacterial locus determining avirulence on both Arabidopsis and soybean. *The Plant Cell*. 3(January):49–59.

Whitham, S., McCormick, S. & Baker, B. 1996. The N gene of tobacco confers resistance to tobacco mosaic virus in transgenic tomato. *Proceedings of the National Academy of Sciences of the United States of America*. 93:8776–8781.

Xiang, T., Zong, N., Zou, Y., Wu, Y., Zhang, J., Xing, W., Li, Y., Tang, X., *et al*. 2008. Pseudomonas syringae Effector AvrPto Blocks Innate Immunity by Targeting Receptor Kinases. *Current Biology*. 18:74–80.

Xiao, S., Brown, S., Patrick, E., Brearley, C. & Turner, J.G. 2003. Enhanced Transcription of the Arabidopsis Disease Resistance Genes RPW8 . 1 and RPW8 . 2 via a Salicylic Acid – Dependent Amplification Circuit Is Required for Hypersensitive Cell Death. *The Plant Cell*. 15:33–45.

Xing, W., Zou, Y., Liu, Q., Liu, J., Luo, X., Huang, Q., Chen, S., Zhu, L., *et al*. 2007. The structural basis for activation of plant immunity by bacterial effector protein AvrPto. *Nature*. 449:243–247.

Yan, S. & Dong, X. 2014. Perception of the plant immune signal salicylic acid. *Current Opinion in Plant Biology*. 20:64–68.

Yang, S. & Hua, J. 2004. A haplotype-specific Resistance gene regulated by BONZAI1 mediates temperature-dependent growth control in Arabidopsis. *The Plant Cell*. 16:1060–1071.

Yoo, S.-D., Cho, Y.-H. & Sheen, J. 2007. Arabidopsis mesophyll protoplasts: a versatile cell system for transient gene expression analysis. *Nature Protocols*. 2(7):1565–1572.

Zhang, Y., Goritschnig, S., Dong, X. & Li, X. 2003. A Gain-of-Function Mutation in a Plant Disease Resistance Gene Leads to Constitutive Activation of Downstream Signal Transduction Pathways in. *The Plant Cell*. 15:2636–46.

Zhang, Z., Wu, Y., Gao, M., Zhang, J., Kong, Q., Liu, Y., Ba, H., Zhou, J., *et al*. 2012. Disruption of PAMP-induced MAP kinase cascade by a pseudomonas syringae effector activates plant immunity mediated by the NB-LRR protein SUMM2. *Cell Host and Microbe*. 11:253–263.

Zhu, Y., Qian, W. & Hua, J. 2010. Temperature modulates plant defense responses through NB-LRR proteins. *PLoS pathogens*. 6.

Zipfel, C. & Felix, G. 2005. Plants and animals: A different taste for microbes? *Current Opinion in Plant Biology*. 8:353–360.